MICRO-BOTTLE RESONATOR FOR LIQUID ETHANOL AND SODIUM HYPOCHLORITE SENSING

NURUL ATIKA BINTI BAHARUDDIN

FACULTY OF ENGINEERING
UNIVERSITY OF MALAYA
KUALA LUMPUR

2022

Universiti Malaya

MICRO-BOTTLE RESONATOR FOR LIQUID ETHANOL AND SODIUM HYPOCHLORITE SENSING

NURUL ATIKA BINTI BAHARUDDIN

DISSERTATION SUBMITTED IN FULFILLMENT OF THE REQUIREMENTS FOR THE DEGREE OF MASTER OF ENGINEERING SCIENCE

FACULTY OF ENGINEERING
UNIVERSITY OF MALAYA
KUALA LUMPUR

2022

Universiti Malaya

UNIVERSITY OF MALAYA

ORIGINAL LITERARY WORK RELATION

Name of Candidate: Nurul Atika Binti Baharuddin

Registration/Matric No: KGA180035, 17068020/2

Name of Degree: Master of Engineering Science

Title of Project Paper/Research Report/Dissertation/Thesis ("this Work"):

Micro-Bottle Resonator for Liquid Ethanol and Sodium Hypochlorite Sensing

Field of Study: Photonics

I do solemnly and sincerely declare that:

(1) I am the sole author/writer of this Work;
(2) This Work is original;
(3) Any use of any work in which copyright exists was done by way of fair dealing and for permitted purposes and any excerpt or extract from, or reference to or reproduction of any copyright work has been disclosed expressly and sufficiently and the title of the Work and its authorship have been acknowledged in this Work;
(4) I do not have any actual knowledge nor do I ought reasonably to know that the making of this work constitutes an infringement of any copyright work;
(5) I hereby assign all and every rights in the copyright to this Work to the University of Malaya ("UM"), who henceforth shall be owner of the copyright in this Work and that any reproduction or use in any form or by any means whatsoever is prohibited without the written consent of UM having been first had and obtained;
(6) I am fully aware that if in the course of making this Work I have infringed any copyright whether intentionally or otherwise, I may be subject to legal action or any other action as may be determined by UM.

Candidate's Signature Date:26012022

Subscribed and solemnly declared before,

Witness's Signature Date:26/1/2022

Name:
Designation:

University of Malaya

MICRO-BOTTLE RESONATOR FOR LIQUID ETHANOL AND SODIUM HYPOCHLORITE SENSING

ABSTRACT

Optical micro-bottle resonator (MBR) structure fabricated based on arc fusion approach was widely deployed to implement highly compact, low cost and versatile sensor device. This dissertation presents an investigation on MBR for liquid ethanol and sodium hypochlorite sensing. The resonator was made of an SMF-28 silica fiber using a new method known as "soften-and-compress" to create a bottle structure. At first, the MBR with a midriff diameter D_b = 170 μm, stem diameter D_s = 125 μm and length L_b = 180 μm was fabricated for use as a liquid sensor to detect ethanol concentration within a range from 10% to 100%. The MBR was characterized by injecting a tuneable wavelength light source through a 3μm bare microfiber and it exhibits a quality factor (Q-factor value) of > 10^4. The shift in the MBR's resonant wavelength was around 6 nm as the ethanol concentration was increased from 10% to 100%. Its performance was compared with a bare microfiber (no-MBR) based sensor. It was found that the MBR ethanol liquid sensor showed a sensitivity of 0.1756 dB/%ppm, linearity of 99.28% and standard deviation of 3.355 dB, which were significantly better than those of the bare microfiber sensor. The sensor maintained a good stability while in operation for over 20 minutes and it remained stable when the experiment was repeated three times. For measuring sodium hypochlorite concentration, another MBR with a bottle diameter (D_b), bottle length (L_b) and stem diameter (D_s) of 180 μm, 183 μm and 125 μm respectively was fabricated using the similar method. A tapered microfiber with 2 μm diameter was used to launch light into the structure and the wavelength gallery modes resonances are observed with a Q-factor of approximately 7.95×10^5. It is obtained that transmitted light power from the MBR reduces with the increases of sodium hypochlorite concentrations from 1% to 6%. The

Universiti Malaya

sensor sensitivity was about 3.7319 dB/%ppm, which is higher than that of the bare microfiber-based sensor. The whispering gallery mode's resonance wavelength also shifted from 1552.203 nm to 1552.213 nm with a sensitivity of 0.002 nm/%ppm linearity of 97.64%, as the concentration increased from 1% to 6%. These results indicate the MBR structure has a great potential for use as a liquid sensor.

Keywords: Micro-bottle resonator, whispering gallery modes, liquid ethanol sensor, sodium hypochlorite sensor

Universiti Malaya

RESONATOR BOTOL MIKRO UNTUK SENSING CECAIR ETANOL DAN HIPOKLORIT NATRIUM

ABSTRAK

Struktur resonator botol mikro optik (MBR) yang direka berdasarkan pendekatan gabungan lengkuk telah digunakan secara meluas untuk melaksanakan peranti penderia yang sangat padat, kos rendah dan serba boleh. Disertasi ini membentangkan siasatan ke atas MBR untuk penderiaan etanol cecair dan hipoklorit natrium. Resonator ini diperbuat daripada serat silika SMF-28 menggunakan kaedah baru yang dikenali sebagai "melembutkan dan memampatkan" untuk mencipta struktur botol. Pada mulanya, MBR dengan diameter bahagian tengah (D_b) = 170 μm, diameter linggi (D_s) = 125 μm dan panjang (L_b) = 180 μm telah direka untuk digunakan sebagai penderia cecair untuk mengesan kepekatan etanol dalam julat antara 10% hingga 100%. MBR dicirikan dengan menyuntik sumber cahaya gelombang yang boleh dilaraskan melalui mikrofiber 3 μm dan ia mempamerkan faktor kualiti (nilai Q-faktor) > 10^4. Peralihan gelombang resonan MBR adalah sekitar 6 nm kerana kepekatan etanol ditingkatkan daripada 10% kepada 100%. Prestasinya dibandingkan dengan penderia berasaskan mikrofiber (tiada-MBR). Didapati bahawa penderia cecair etanol MBR menunjukkan kepekaan 0.1756 dB/%ppm, kelelurusan 99.28% dan sisihan piawai 3.355 dB, yang jauh lebih baik daripada penderia mikrogentian terdedah. Penderia mengekalkan kestabilan yang baik semasa beroperasi selama lebih dari 20 minit dan ia kekal stabil apabila eksperimen diulang sebanyak tiga kali. Untuk mengukur kepekatan hipoklorit natrium, satu lagi MBR dengan diameter botol (D_b), panjang botol (L_b) dan diameter linggi (D_s) masing-masing 180 μm, 183 μm dan 125 μm masing-masing direka menggunakan kaedah yang sama. Mikrogentian tirus yang ditumbuk dengan diameter 2 μm digunakan untuk melancarkan cahaya ke dalam struktur dan mod ruang panjang gelombang salunan diperhatikan dengan faktor Q kira-

Universiti Malaya

kira 7.95×10^5. Ia diperolehi bahawa kuasa cahaya yang dihantar dari MBR mengurang dengan peningkatan kepekatan hipoklorit natrium dari 1% hingga 6%. Kepekaan deria adalah kira-kira 3.7319 dB/%ppm, yang lebih tinggi daripada penderia berasaskan mikrogentian terdedah. Gelombang salunan mod ruang berbisik juga berubah daripada 1552.203 nm kepada 1552.213 nm dengan sensitiviti 0.002 nm/%ppm kelelurusan 97.64%, kerana kepekatan meningkat daripada 1% kepada 6%. Keputusan ini menunjukkan struktur MBR mempunyai potensi besar untuk digunakan sebagai penderiaan cecair.

Kata kunci: Resonator mikro-botol, mod ruang berbisik, penderia etanol cecair, penderia hipoklorit natrium

Universiti Malaya

ACKNOWLEDGEMENT

First and foremost, this thesis has benefited greatly from the support of many people whom I would like to sincerely thank them here:

To my Master Research supervisors, Dr Norrima Binti Mokhtar and Prof Ir Dr Sulaiman Wadi Harun for giving me a chance to do research on such interesting topic. They have continuously guiding, giving invaluable suggestions and advice not limited to research area, and their constant support which push forwards my research progress. I may have been led astray if not for their tremendous guidance.

To all my seniors from the same department which have constantly guiding me from day-1 in the optic laboratory and teach me on handling and familiarize the process especially to Dr Md Ashadi Md Johari. My gratitude goes to Prof Kaharuddin for teaching me in Research Methodology class which have been a great start on my research journey. To all staff from Faculty of Engineering which have been very helpful and assistive in handling matters regarding my program.

To my colleague from Adecco and ACASIA, thank you for being supportive and understanding throughout my studies journey.

Finally, I would like to thank my parents, Mrs Alida Binti Loop, Mr Baharuddin Bin Ibrahim, my siblings, Nurul Adira Binti Baharuddin, Muhammad Nuzul Naim Bin Baharuddin and Mar Amieyra Mohd Rejab for always been at my side throughout the joyous and difficult times of research journey.

Universiti Malaya

TABLE OF CONTENTS

Universiti Malaya

Universiti Malaya

LIST OF FIGURES

Universiti Malaya

Universiti Malaya

LIST OF TABLES

Universiti Malaya

LIST OF SYMBOLS AND ABBREVIATION

CO_2	:	Carbon Dioxide
CaF_2	:	Calcium fluoride
CQED	:	Cavity Quantum Electro-Dynamics
EtOH	:	Ethanol
FSR	:	Free Spectral Range
MBR	:	Micro-Bottle Resonator
NaOCl	:	Sodium Hypochlorite
OH	:	Hydroxyl
OMR	:	Optical Micro-Resonator
OPM	:	Optical Power Meter
Q-factor	:	Quality-factor
RH	:	Relative Humidity
RI	:	Refractive Index
SMF	:	Single Mode Fiber
TE	:	Transverse Electric
TIR	:	Total Internal Reflection
TLS	:	Tuneable Laser Source
WG	:	Whispering Gallery
WGM	:	Whispering Gallery Mode
WKB	:	Wentzel-Kramers-Brillouin
ZnO	:	Zinc Oxide

Universiti Malaya

CHAPTER 1 : INTRODUCTION

1.1 Background

Optical micro-resonators (OMRs) are microscopic structures capable of confining lighting small spaces(Del'Haye et al., 2007). The optical confinement causes to the generation of resonant electromagnetic modes, which show as narrow lines in their spectra. They are an exciting new field of research that has gained tremendous interests in recent years due to their easy fabrication and excellent integration capability as well as their many potential applications in photonic devices (Vollmer & Yang, 2012). They are widely employed in sensing application due to the sensitivity of the optical modes to external perturbations. The sensitivity of OMRs enhances as the linewidth of their resonant features reduces. This linewidth is proportional to the optical losses, and it is inversely proportional to the Q-factor quantity of the resonator. The Q-factor is defined as $Q = \lambda_0/\Delta\lambda$, where λ_0 is the resonant wavelength, and $\Delta\lambda$ is its linewidth.

The lowest intrinsic losses could be obtained in whispering gallery mode (WGM) based on OMR. In this type of resonators, the light is confined by total internal reflection (TIR) in a dielectric structure with an axisymmetric cross-section. The resonant photons are confined in a microscale resonator for long periods of time in the WGM based OMR and this light-matter interaction could be strongly enhanced. This makes this device to be an ideal platform for sensitive detection in various sensors (Ding et al., 2012). For instance, Vollmer et al. proposed the WGM microsphere-based sensor for the detection of proteins in aqueous environments by monitoring the resonant frequency shift(Vollmer et al., 2002). Since then, the WGM microspheres has become the most used WGM OMRs for sensing applications(S. Chu et al., 1999; Liang et al., 2018). This is due to their straightforward fabrication and reasonably high Q-factors. However, many other WGM

Universiti Malaya

structures including rings(White et al., 2006), disks(Eryürek et al., 2017), cylinders (Yang et al., 2013) and tubes (Kazanov et al., 2018) were also reported.

In this work, whispering gallery modes in optical micro-bottle resonator, a less explored geometry is investigated for sensing application. The optical micro-resonators studied in this dissertation are called micro-bottle resonators (MBR) because their profile often resembles an elongated spheroid or a microscopic bottle. Figure 1.1 shows an illustration of MBR, which was constructed based on deformation of a cylinder along its long axis. As shown in the figure, the radius of the cylinder increases smoothly up to a maximum, to then decrease again to form a bottle structure. The MBR structure is capable to combine whispering gallery modes (WGMs) with "bouncing ball" modes, featuring caustics that limit the propagation about the axial direction. The idea of using a micro-bottle geometry or bulge structure to fully confine light was brought up by Murugan et. al.(Murugan et al., 2009) in 2009. OMRs have some advantages over microsphere-based resonators, such as ease of coupling using tapered microfiber, the possibility of obtaining a large number of equally-spaces modes in the spectrum and fast tunability by the application of strain (Louyer et al., 2005; Pöllinger et al., 2009).

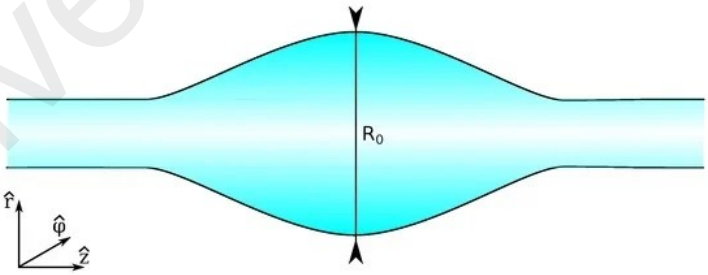

Figure 1.1: MBR structure (Bianucci, 2016)

Micro-bottle resonator (MBRs) is one of the micro resonators which gained plenty of interest recently. This new class of whispering gallery modes resonator has captured much intention due to the structure, the size and also its capability in sensing application. The MBRs are created from the silica fiber using a method so called "heat-and-pull" in

Universiti Malaya

order to produce a bubble structure in the midriff area (Kakarantzas et al., 2001) (Ward et al., 2006; Warken et al., 2008). Later, the thermo technique known as "soften-and-compress" were used to create bulge on the silica fiber. The fiber is heated in certain temperature and compressed periodically from the both sides to form bottle structure(Murugan et al., 2009). The capability to remain the existing of whispering gallery modes along the smooth surface bent structure made this resonator special. Hence, by combining the WG-ring and WG bouncing-ball principle, the MBRs are able to support true 3D light confinement. While other form of resonator only supported 2D light confinement, this has made MBRs more unique (Sumetsky, 2004a). The area of whispering gallery modes modal confinement defined by two MBRs turning points (Louyer et al., 2005). MBRs are competent to sustain a whispering gallery mode with smaller magnitude-order of free-spectral range (FSR) than the same diameter of microsphere (Murugan et al., 2009).The survival of whispering gallery modes through the radius of MBRs became more accessible because of the size are in nanoscale (Sumetsky et al., 2011) . It is easy to trap light to make it close to its surface. The quality factor of the MBRs are defined by calculation from the experimental values and has been demonstrated in several prior research (Murugan et al., 2011).

1.2 Motivation of Study

The WGM OMR was proposed recently and has been extensively studied theoretically and experimentally (Chiasera et al., 2010). However, micro-bottle is less explored geometry for WGM sensors. MBR is a highly oblate resonator, which can sustain non-degenerate WGMs that exhibit two well separated spatial regions with enhanced field strength, corresponding to modal turning points. The free spectral range (FSR) of MBRs is predicted to be about one order of magnitude smaller than that of microsphere resonators of equal diameter (Liang et al., 2018). Furthermore, the MBR

Universiti Malaya

structure could efficiently combine light spatially and temporally, resulting in large optical Q-factor and small mode volume, yielding long photon lifetime and high optical intensity. These characteristics are particularly useful in many applications including compact optical elements, cavity quantum electro-dynamics (CQED), narrow linewidth micro-lasers, add-drop filter and biosensors (Louyer et al., 2005; Sumetsky, 2017; Sumetsky et al., 2011; Yin et al., 2018). So far, MBRs have been fabricated primarily by “heat-and-pull” techniques, using modified fibre tapering machine(Warken et al., 2008). This study explores on preparing optical MBR based on a simpler method so-called ``soften-and-compress" to create a bulge (bottle) structure for sensing applications.

1.3 Objectives of Study

This work aims to explore whispering gallery modes in optical micro-bottle resonator (MBR) for sensing applications. To achieve this, the following objectives have been outlined to guide the research path.

i. To fabricated and characterized micro-bottle resonator (MBR)
ii. To apply the newly developed MBR structure for liquid ethanol sensing
iii. To apply the MBR structure for sodium hypochlorite sensing

1.4 Dissertation Overview

Chapter 1 introduces this research work where the background, motivation and objectives of this study were discussed. Chapter 2 presents the literature review pertaining to the research works. The theory, working principle and fabrication of optical micro-resonators including whispering gallery mode and micro-bottle resonators as well as a microfiber are discussed in this chapter. Chapter 3 presents an investigation on optical micro-bottle resonator (MBR) for liquid ethanol sensing. The MBR was made of an SMF-28 silica fiber using a new method known as “soften-and-compress” to create a bottle

Universiti Malaya

structure. It was characterized by injecting a tunable wavelength light source through a 3μm bare microfiber. The fabricated MBR was then used as a liquid sensor to detect ethanol concentration within a range from 10% to 100% by monitoring the shift in the MBR's resonant wavelength and the transmitted light power from the resonator. In Chapter 4, MBR based sensor is proposed and demonstrated for measuring sodium hypochlorite concentration. The transmitted light power from the MBR and MBR's resonant wavelength were investigated as the sodium hypochlorite concentration was varied from 1% to 6%. The finding of this research work is summarized and concluded in Chapter 5.

Universiti Malaya

CHAPTER 2 : LITERATURE REVIEW

2.1 Introduction to Optical Micro-Resonator

Optical micro-resonator (OMR) is a microscopic formation to efficiently confine light in small areas (Vahala, 2003a). The optical detention inside the resonator leads to the development of resonant electromagnetic modes, which is demonstrated as a narrow resonance line in the output spectrum. The recent most promising applications of OMR is in label-free sensing since the generated optical modes are sensitive to external agitations. In general, the sensitivity of the resonant based sensor increases whenever decreasing trend showed in the linewidth of their resonant wavelength. These optical losses are defiantly proportional to the linewidth, which is in reverse proportional to the quality factor (which is a defined as $Q = \lambda_0/\Delta\lambda$, where λ_0 is the midriff wavelength of the depth resonance and $\Delta\lambda$ was a linewidth). The whispering gallery mode (WGM) is defined as a confined of light by total internal reflection concept in a dielectric micro-resonator structure with a cross-section (axisymmetric). It was shown to have the lowest intrinsic losses among OMRs (Matsko & Ilchenko, 2006a). This low loss characteristic allowed the WGM based OMR to have extremely sensitive detection which lead to be good sensor (Foreman et al., 2015). Several WGM based OMRs have been reported recently in different geometries such as ball, cylindrical, spheres, rings, disks, etc. The recent best Q-factor value have been recorded is 10^{11} by crystalline CaF_2 WGM resonators (Savchenkov et al., 2007). However, due to low cost and simplicity of processing, silica fiber has marked as the most popular material to be used as resonator, which able to have Q-factor as high as 10^{10} (Gorodetsky et al., 1996). The WGM micro-disks planar structure reported a Q-factor of 10^9 (Lee et al., 2012). Based on the performance (Q-factor), reasonable fabrication and easy handling, the WGM microsphere resonator has been widely used for sensing purpose. However, compare to other resonator

Universiti Malaya

structures, the micro-bottle resonator (MBR) received less explored structure to be used as sensor.

2.2 Whispering Gallery Mode (WGM) OMR

Recently, OMRs have received tremendous interests due to their huge potential applications in many areas including bio-sensing, nonlinear optics, optical communication, and laser technology (Almeida et al., 2004; Armani et al., 2007) (S. T. Chu et al., 1999; Del'Haye et al., 2007; Djordjev et al., 2002). The light confinement, Q-factor (Q) and mode volume (V) in OMR could be improved by employing whispering gallery mode (WGM) resonators(Vahala, 2003b). This is due to the strength of coupling in OMR is depending on the ratio of Q-factor and mode volume and whispering gallery modes was reported to have the highest value of Q/V so far. The standard WGM optical micro-resonator such as microsphere and micro-disks confines the light along the resonator surface by continuous total internal reflection (Kippenberg et al., 2004; Matsko & Ilchenko, 2006a).

One of the advantages of WGMs in a small mode volume is capability to have wide spacing of frequency between repeated modes. Due to the monolithic structure, WGM micro-resonator could experience some limited tuning range. This is one of the reasons why bottle structure of WGM micro-resonator received so much intention; because its capability to customize the mode structure while maintain the ratio of Q/V (Kakarantzas et al., 2001). Figure 2.1 shows the MBR, which allows a bundle of modes to be confined by total internal reflection. These modes were oscillated along the resonator axis between two turning point which known as angular momentum barrier (Louyer et al., 2005). The subsequent hub standing wave structure shows a fundamentally upgraded power at the supposed "caustics" of the container mode, situated at the defining moments of the consonant movement. The MBR has an equidistant range of eigenmodes

Universiti Malaya

marked by the ‘‘azimuthal quantum number’’ m, which checks the quantity of wavelengths that fit into the perimeter of the resonator, and the ‘‘axial quantum number’’ q, which counting the axial intensity nodes numbers (Louyer et al., 2005) . The frequency spacing between modes would be known as axial (azimuthal) free spectral range (FSR). For small structure of WGM resonator, the value of the azimuthal FSR would be very large. In some cases, by changing the diameter of the resonator, it will change the resonant frequency up to 1% of the optical frequency. However, tuning a WGM micro-resonator to become large diameter could be specified as a critical issue. Refractive index on the silica fiber and temperature would remain the importance properties should be under consideration. It was reported in some experiments that the numbers of azimuthal FSR could be increased up to 35% by changing the diameter up to 75 μm. However, there is another tuning process which involve the mechanical strain, where the diameter and the refractive index of the resonator were totally changed. This mechanical strain technique (tuning over $400QHz$) could increase the azimuthal FSR up to 50% where the diameter is increased up to $80\mu m$. Unfortunately, this bottle resonator have some disadvantages where the axial FSR totally depending on the curve of the bottle and it could decrease the numbers on its azimuthal FSR if the curve of bottle formed in bad condition (Louyer et al., 2005). Therefore, it is importance to have a sufficient tuning the bottle resonator properly; so that the axial FSR could remained the resonance frequency respectively.

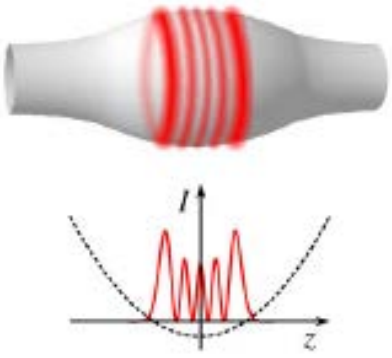

Figure 2.1: Bundle of modes confined by total internal reflection on WGM (Pöllinger et al., 2009).

Universiti Malaya

2.3 Theory of MBR

Micro-bottle resonators (MBRs) are a type of WGM resonators, essentially cylindrically symmetric dielectric structures processing a uniform dielectric constant (we are ignoring the effects of material dispersion). The radius changes (symmetrically with respect to the origin in an ideal bottle) with the axial position, as *R*(z). If the variation in radius is very small (i.e., $dR/dz << 1$), then the mode structure can be studied analytically. The first solution for the eigenfrequencies of MBRs was found by taking the Wentzel-Kramers-Brillouin (WKB) approximation (Sumetsky, 2004b). However, another method, which was typically used for WGM resonators and can give explicit expression for the fields, will be discussed here (Louyer et al., 2005). The following equations are the Maxwell's equations in a uniform, source free for harmonic fields oscillating with an angular frequency ω.

$$\vec{\nabla} \cdot \vec{D} = 0, \quad \vec{\nabla} \times \vec{E} = iw\vec{B},$$

$$\vec{\nabla} \cdot \vec{B} = 0, \ \vec{\nabla} \times \vec{H} = -iw\vec{D}. \tag{2.1}$$

Taking the curl of the curl equations, using vector calculus identities and the constitutive relations $\vec{D} = \epsilon\vec{E}$ and $\vec{B} = \mu\vec{H}$, the following two uncoupled Helmholtz equations for the electric ($\vec{E}$) and magnetic ($\vec{H}$) fields can be obtained:

$$\nabla^2\vec{E} + k^2\vec{E} = 0, \tag{2.2}$$

$$\nabla^2\vec{H} + k^2\vec{H} = 0, \tag{2.3}$$

where $k^2 = \mu\epsilon\omega^2$. While the equations are uncoupled, the fields are still coupled by the transversality requirement that holds in a uniform source-free geometry,

$$\omega\mu\vec{H} = \vec{k} \times \vec{E}, \tag{2.4}$$

where $\vec{k}$ is the wavevector with magnitude k pointing along the direction of propagation. It is possible in some cases, to solve these equations including full polarization information, but it is simpler to take advantages of the bottles' quasi-cylindrical geometry

Universiti Malaya

and focus on the experimentally relevant modes whose electric field is oriented along the long axis of the bottle (so that $E = E\,\hat{z}$, usually denoted as transverse electric (TE) polarization). Under this condition, Equation (2.2) reduces to a scalar Helmholtz equation,

$$\nabla^2 E + k^2 E = 0, \tag{2.5}$$

and the magnetic field can be calculated (if desired) from the transversality Equation (2.4).

Equation (2.5) can be solved in cylindrically symmetric systems by separation of variables, assuming that $E(r, \varphi, z) = f(r, z)e^{im\varphi}$ (m is an integer azimuthal mode number). Thanks to the slow variation of the radius, it is a good approximation to split on the radial and axial coordinates, $f(r, z) = F(r)Z(z)$, so that,

$$E(r, \varphi, z) = F(r)Z(z)e^{im\varphi}. \tag{2.6}$$

By putting Equation (2.6) back into Equation (2.5), two separate equations for the radial and axial dependence can be found,

$$\frac{d^2R}{dr} + \frac{1}{r}\frac{dR}{dr} + \left[k_\perp^2(z) - \frac{m^2}{r^2}\right]R = 0, \tag{2.7}$$

$$\frac{d^2Z}{dz^2} - k_\perp^2(z)Z = -k^2 Z, \tag{2.8}$$

where $k_\perp$ and k_z are the transverse and axial components of the wavevector, satisfying that,

$$k_\perp^2(z) + k_z^2(z) = k^2. \tag{2.9}$$

These equations are still coupled due to the z-dependency of the wavevector components, so we need to finish uncoupling them. This is simplest to do if we restrict ourselves to “fundamental” WGM modes, the ones with a trajectory lying closest to the surface. Under this condition, we can neglect the radial component of the wavevector; thus, $k_\perp = k_\varphi$, and

$$k = \sqrt{k_\varphi^2 + k_z^2} = \frac{2\pi n}{\lambda_0}, \tag{2.10}$$

Universiti Malaya

where λ_0 and n is the vacuum wavelength and the resonator's index of refraction, respectively.

Due to the symmetry of revolution, the z-component of the angular momentum should be conserved. It requires the product $k_\varphi(z)R(z)$ to be a constant. Since, at the caustics ($z = \pm z_c$), it is known that there is no propagation along the z axis, then $k_\varphi(\pm z_c) = k$, and

$$k_\varphi(z) = \frac{kR_c}{R(z)} = \frac{m}{R(z)}, \tag{2.11}$$

where $R_c = R(\pm z_c)$ is the radius of the microbottle at the caustics, and $kR_c = m$. Now, these relations in Equation (2.8) can be used to obtain the equation for the axial dependence in terms of the micro-bottle profile $R(z)$,

$$\frac{d^2Z}{dz^2} - \left[\frac{m}{R(z)}\right]^2 Z = -k^2 Z, \tag{2.12}$$

Equation (2.12) can be rewritten as a Schrödinger-like equation as follows:

$$-\frac{d^2Z}{dz^2} + V_{eff}(z)Z = E_{eff}Z, \tag{2.13}$$

with

$$V_{eff}(z) = \left[\frac{m}{R(z)}\right]^2, \; E_{eff} = k^2. \tag{2.14}$$

An analytic solution can be found to this equation if we choose a quasi-parabolic spatial profile,

$$R(z) = \frac{R_0}{\sqrt{1+(\alpha^2 z^2)}} \approx R_0\left(1 - \frac{\alpha^2 z^2}{2}\right). \tag{2.15}$$

Then, Equation (2.13) becomes that of a simple harmonic oscillator with an energy shift m^2/R_0^2,

$$-\frac{d^2Z}{dz^2} + \left(\frac{1}{2}\Delta E_m + \frac{m^2}{R_0^2}\right) = k^2 Z, \tag{2.16}$$

where $\Delta E_m = \sqrt{2}m\alpha/R_0$.

The possible wavevectors are now given by the eigen energies of the harmonic oscillator plus the energy shift:

Universiti Malaya

$$k_{mq}^2 = \frac{m^2}{R_0^2} + \left(q + \frac{1}{2}\Delta E_m\right), \tag{2.17}$$

where q represents a natural axial mode number. The corresponding solution for the z-dependence of the field is then given by:

$$Z_m q(z) = C_{mq} H_q\left(\sqrt{\frac{\Delta E_m}{2}}z\right) e^{-\frac{\Delta E_m}{4}z^2}, \tag{2.18}$$

with $H_q(x)$ is the Hermite polynomial of degree q with a normalization constant

From the above discussion, it can be found that the MBR profile will directly influence the z-dependence of the electric field, and the spectral distribution of the different axial modes. A slowly changing parabolic profile for the micro-bottle will then result in approximately equispaced axial resonant modes in its spectrum.

Based on Equation (2.10), Equation (2.7) can be rewritten as a Bessel differential equation with a parametric dependence on z via $k_\varphi(z)$, to solve for the radial dependence.

$$\frac{d^2R}{dr} + \frac{1}{r}\frac{dR}{dr} + \left[k_\varphi^2 - \frac{m^2}{r^2}\right]R = 0. \tag{2.19}$$

The radial dependence will then be given by Bessel functions of the first, second, or third kind. The details will depend on the number of interfaces between the resonator and the outside medium; that is, whether the micro-bottle is solid or hollow.

For a solid micro-bottle, there is a single interface, so (for a given azimuthal order m) the solution can be separated in two parts – one inside the bottle and one outside, assuming a refractive index n_0 for the medium:

$$R(r,z) = \begin{cases} A_m J_m(k_\varphi r), & r \le R(z) \\ H_m^{(1)}\left(\frac{n_0}{n}k_\varphi r\right) + B_m H_m^{(2)}\left(\frac{n_0}{n}k_\varphi r\right), & r > R(z) \end{cases}. \tag{2.20}$$

On the inside, the field is proportional to a Bessel function (to avoid a singularity at the origin), while on the outside, it is a linear combination of Hankel functions of the first and second kind, which asymptotically approach outgoing and incoming cylindrical waves at very large distances, respectively. Requiring continuity of the field and its derivative for each $R(z)$, we can obtain expressions for the coefficients.

Universiti Malaya

2.4 Fabrication of Optical MBR

MBR can be fabricated by forming a deformation along a cylindrical silica rod where the bump structure is made in the midriff of it. The radius of silica rod increases smoothly up to maximum and decrease gradually to form a symmetrical bottle structure. This structure functions to combine the "bouncing ball" modes with the WGMs around the bump structure and introducing caustics that limit the wave propagation in the axial direction. With routine stable propagation, it would achieve high Q-factors value as high as 10^7. Most of the MBRs are based on optical fibers; thus, their fabrication tends to be straightforward, without requiring microfabrication equipment. This simplicity is greatly appreciated in a research environment, but it implies that the fabrication throughput is low.

In general, fiber-based MBR have not yet been shown to be amenable to mass-production. The initial method used for their fabrication involves thermal softening and pulling. This involves heating up an optical fiber until its softening point of around 1500^{o}C, generally accomplished using a flame (Birks & Li, 1992) , a gas laser (Ward et al., 2006) , or a ceramic heater (Ding et al., 2010) and then mechanically pulling it to reduce its size. First, the fiber is softened by a localized source of heat and pulled to a desired starting diameter. Then, this step is repeated at another location, resulting in the creation of a bulge in the optical fiber. This technique produced a MBR with a relatively low Q-factors (Ding et al., 2010) , but the Q-factors can be improved in the order of 10^7 and 10^8 with technical improvements (Bianucci et al., 2010) .

The micro-bottle structure can also be obtained by reversing the mechanical motion with a "soften and compress" method instead of "heating and pulling"(Murugan et al., 2009) . In this approach, a continuous piece of silica fiber is heated in a controlled fashion while it is being compressed. The compression of the softened fiber then results

Universiti Malaya

in a bulge structure with good control of the geometry. A MBR with a Q-factors close to 10^6 can be achieved by this technique. This method has the advantage of being able to be applied in a straightforward fashion using a commercially available fusion splicer, reducing the need for custom motion stages in a MBR fabrication setup. However, it can be difficult to implement if the desired diameter of the micro-bottle is significantly smaller than that of standard optical fiber.

Glass is not the only material that has been used to fabricate MBRs. Gu et al. employed an ultraviolet (UV)-curing epoxy to form droplets on an optical fiber that self-assemble into micro-bottles due to interfacial forces (Gu et al., 2014) ("Fabrication of ultraviolet-curable adhesive bottle-like microresonators by wetting and photocuring," 2014). This MBR showed a Q-factor of near 10^5. Figure 2.2 shows microscope images of MBR fabricated with different methods. In this work, a "soften-and-compress" technique is used for MBR fabrication.

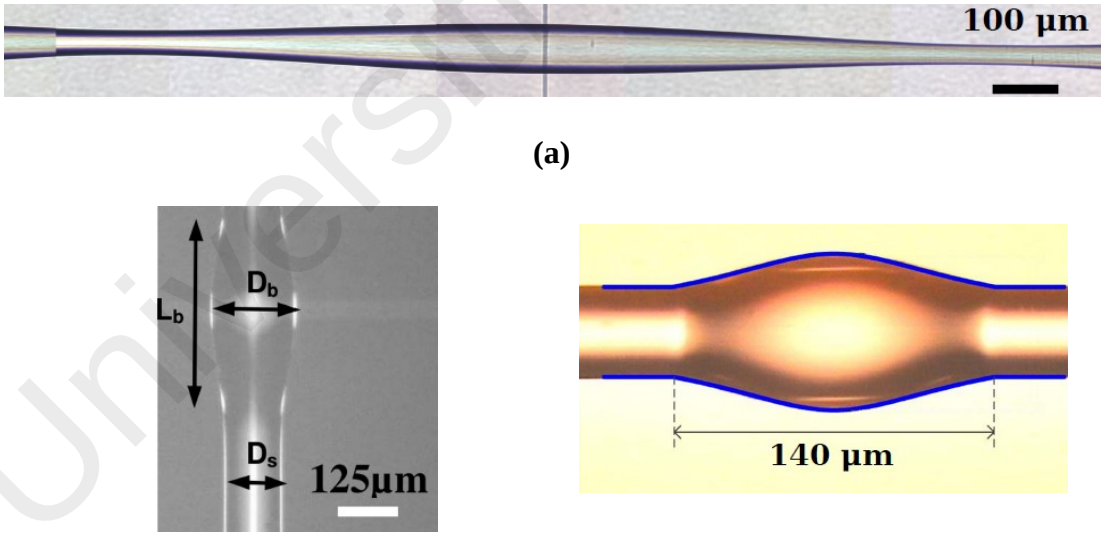

Figure 2.2: Microscope images of MBR fabricated with different methods: (a) "heating and pulling" (Ward et al., 2006) (b) "soften-and-compress" (Murugan et al., 2009) and (c) Epoxy-based MBR (Gu et al., 2014)

Universiti Malaya

2.5 Modes and Fields Behaviour of Optical MBR

Rather than 2D light-confinement of microspheres, MBRs achieve a 3D light-confinement structure through their mix of whispering-gallery and bouncing-ball containment impacts. Figure 2.3 delineates the rule of a whispering-gallery MBR (Sumetsky, 2004b)Light imprisonment in such a structure, assigned in tube shaped directions (z,ρ,φ), can be ventured into 2D whispering-gallery beams moving in the plane (ρ,φ) ordinary to the fiber hub z and 2D ricocheting ball beams moving in the plane (z,ρ).

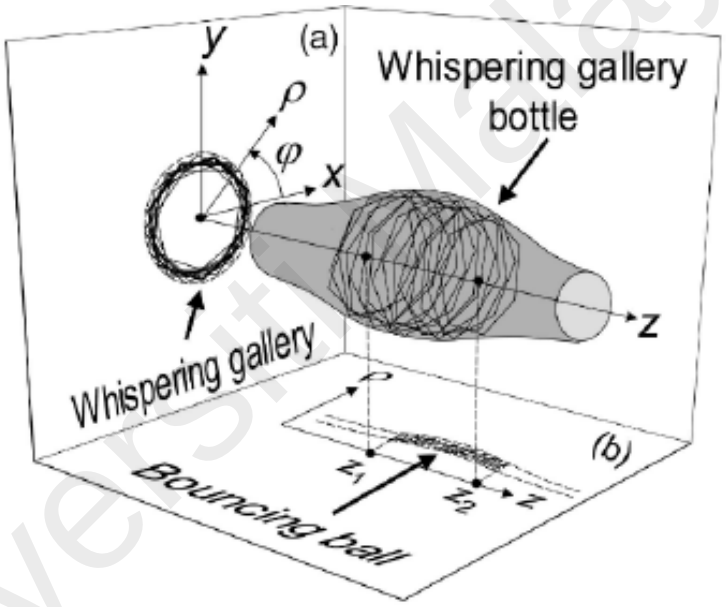

Figure 2.3: The MBR whispering-gallery modes MBR in the projection of plane (ρ, φ) (a), and plane (z, ρ) (b) (Sumetsky, 2004b)

For the full-scale wave condition computation of whispering-gallery MBRs on a dielectric structure, light repression through the mix of tropical WGMs and two defining moments along the resonator pivot ought to be considered. Figure 2.3 represents the idea of MBRs imprisonment where (a) light would winding to and from between two defining moments that are isolated by a separation $2z_c$, and (b) along a tropical whispering-gallery.

University Malaya

Such modes show two spatially isolated caustics (brought about by precise force boundary) situated at $\pm z_c$ with upgraded field quality.

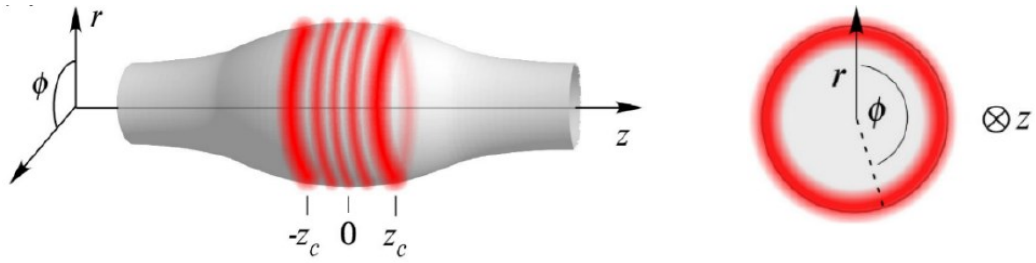

(a) **(b)**

Figure 2.4:The MBR geometry placed along (a) and in a plane (b) perpendicular to the resonator axis (Louyer et al., 2005) .

2.6 Evanescent Wave

An optical fiber consists of two main sections which is core and cladding. Compared to the cladding, the core is designed to has a higher refractive index (RI) to ensure total internal reflection (TIR) under certain conditions based on Snell law. TIR occurred when incident angle (θ_i) is greater than critical angle (θ_c) which cause the light reflection back from core to cladding surface as illustrated in Figure 2.4. However, there is always small portion of energy that penetrates the interface of core and cladding medium during the TIR. This energy is referred to evanescent field as shown in the inset of Figure 2.4.

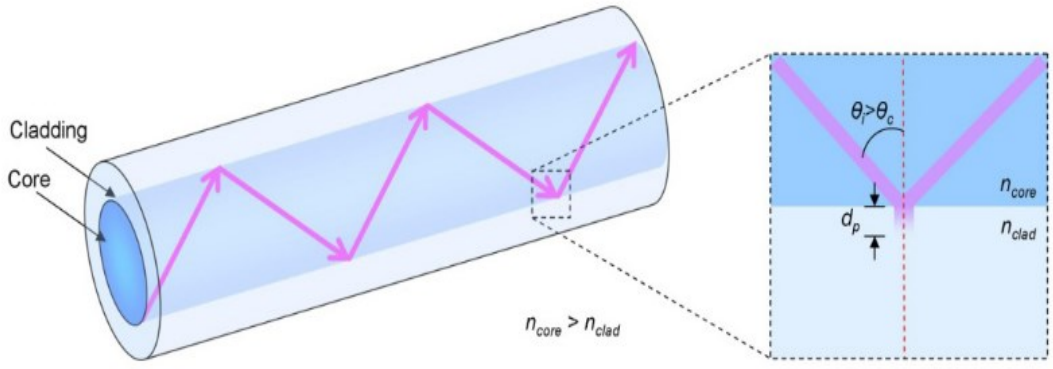

Figure 2.5: Evanescent field generation during TIR (Punjabi et al., 2015)

Universiti Malaya

It was reported that magnitude of the evanescent field increases when the normalised wavelength (ƛ/r) and surrounding refractive index increases (Brambilla, 2010a) . r is the radius of the core. Figure 2.6 shows the relationship between the fraction of power (η_{EF}) in the evanescent field of a silica fiber against the normalized wavelength. It is shown that the fraction of power propagating in the evanescent field depends on the ratio of λ/r. It indicates that the η_{EF} increases monotonically as the ƛ/r increases. Hence, an optical fiber with a smaller core radius would produce larger evanescent wave fractional power.

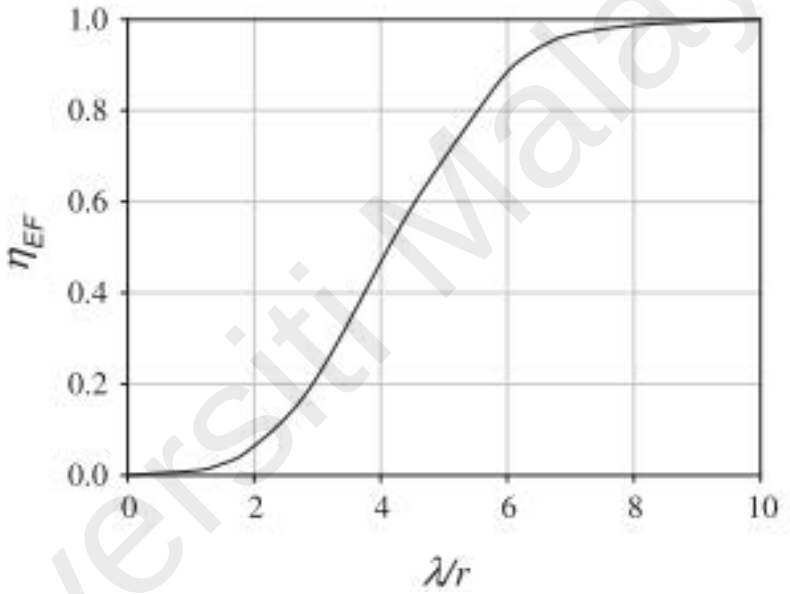

Figure 2.6: Relationship between fraction of power(η_{EF}) in the evanescent wave of the silica fiber and the normalised wavelength (ƛ/r) (Brambilla, 2010a)

The type and number of modes propagating through the fiber could be determine by the physical characteristics of the fiber such as core diameter, refractive index, and operating wavelength. The low amplitude of the evanescent field in a normal SMF could be enhanced by tapering (Mignani et al., 1998) in order to increase interaction of analyte around the taper region with the transmitted light (Bobb et al., 1990) as shown in Figure 2.6. The evanescent field interacts with any surrounding environmental change which

Universiti Malaya

makes it suitable for sensing application. Generally evanescent wave-based sensor could be categorized into two sensing mechanisms: refractometric and absorption. For refractometric type, the device is commonly surrounded by a fluid. Any change in the fluid properties would be translated into respective change of refractive index. Whereas for absorption type, the light intensity travelling the sensing region is recorded when there is change in the fluid properties due to its absorption.

The surface of the optical fiber can be pre-treated with any sensitive material which act as receptors or binding sites for any specific analyte (Chao & Guo, 2006) . Based on Figure 2.7, the sensitive area has a large fraction of power propagating outside the tapered fiber physical boundary and overlaps with the surrounding environment. Any changes in surrounding properties result in a change in output. To increase the sensor detection capability, the sensitive area could be coated with material which react with specific chemical.

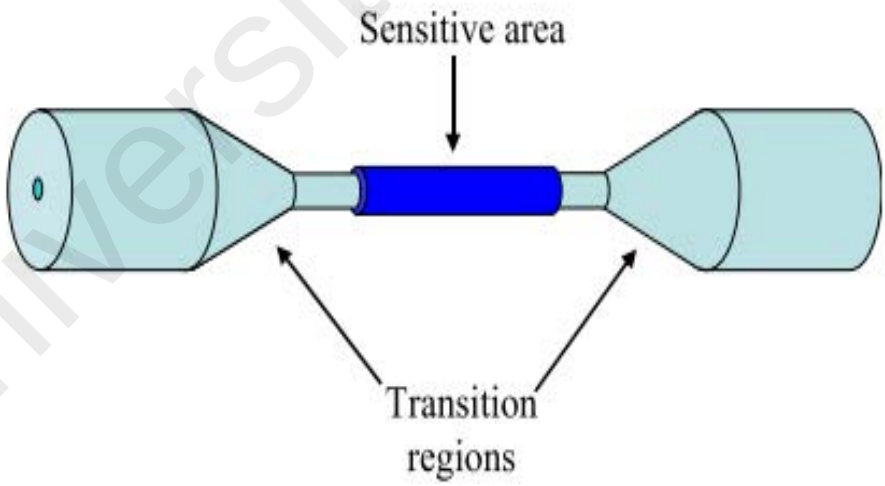

Figure 2.7: Sensitive area has a large fraction of power propagating to interact with the surrounding environment. (Brambilla, 2010a)

Universiti Malaya

2.7 Microfiber

Microfibers exhibit unique characteristics such as large optical confinement, configurability, flexibility, strong optical confinement and large evanescent field which make them suitable for physical sensing such as hydrogen detection, ultra-sensitive surface absorption spectroscopy, chemical and refractive index sensor(Chen et al., 2013) . Large evanescent field propagates outside the microfiber has caused the microfiber to be very sensitive to a change in the surrounding refractive index(Lim et al., 2012a) . The surrounding material's refractive index would increase when the power fraction propagating in the evanescent field increases. It has good evanescent coupling with other waveguides such as metal, semiconductor, and substrate as well as display strong near-field interaction with its surrounding. Thus, high fractional evanescent field allow great responses towards humidity sensing.

Microfiber offers several interesting optical and mechanical properties such as strong evanescent field. Fractional power propagates in the evanescent field outside the physical boundary of the small radii microfiber. This property is essential to fabricate high Q resonators as well as to launch light into high Q micro-resonators (Brambilla, 2010b) . Microfiber also exhibits strong near-field interaction with its surrounding(Wu & Tong, 2013) . It has good evanescent coupling between the microfiber and the other waveguides such as substrates, semiconductor (Ding et al., 2009) , planar waveguide(Armani et al., 2003) and metal. This lead to plenty of new optical devices such as lasers(Jiang et al., 2006) , sensors(Liang et al., 2005) and resonators(Sumetsky et al., 2005) .

Besides that, microfiber is very sensitive to momentum change of photon guide through by mechanical displacement or vibration mass due to its small mass. This enable a development of compact opto-mechanical component/devices. It also allows a low loss propagation when light passing through sharp bends. Therefore microfiber could realize

Universiti Malaya

a compact devices with faster response, lower power consumption and smaller footprints ("Optical microfibers and nanofibers," 2013). Microfiber is fabricated by stretching optical fibre until reaching the desired waist diameter while preserve the original fiber dimensions at their input and output ends. This enables a low loss splicing to interconnect with other standard size optical fibers.

Several methods have been developed to fabricate glass microfiber. The first method is called a self-modulated taper drawing. It requires two-step process: first the SMF is tapered to a diameter of few μm using conventional flame brushing technique. Then the microfiber is broken into two parts and one fiber pigtail is wrapped onto a small hot sapphire rod and the microfiber is further drawn into sub-micron diameter. Subsequently, the sapphire tip is heated using a flame at a distance from the fiber to confines the heat in a small volume and stabilize the temperature distribution("Optical fiber nanowires and microwires: a review," 2010). Even though this fabrication technique is quite complicated, it is capable to produce a microfiber with radius as small as 10 nm("Self-modulated taper drawing of silica nanowires," 2005).

The second method is based on a direct drawing from the bulk glass material. This technique required a small sapphire rod to be heated and placed in contact with bulk glass. This results in a localized softening to the bulk glass. As the sapphire rod is abruptly moved away, a glass filament with diameter of micrometric is formed("Optical fiber nanowires and microwires: a review," 2010). It has advantages in term of flexibility and low-cost equipment. However, the diameter and uniformity of the microfiber is highly difficult to control. It has been widely used to fabricate microfiber from phosphate glasses, tellurite and polymers("Photonics nanowires directly drawn from bulk glasses," 2006).

The third method is based on flame brushing technique, which was previously introduced to fabricate a fiber coupler("Low-loss highly overcoupled fused couplers:

Universiti Malaya

Fabrication and sensitivity to external pressure," 1988). It is done by applying small flame movement under a stretched optical fiber. The optical fiber extremities and burner are hold by stages and connected to the computer. An highly accurate microfiber could be fabricated by precisely controlled the flame movement("The shape of fiber tapers," 1992). It could produce microfibers with radius as small as 30 nm("Fabrication of optical fibre nanowires and their optical and mechanical characterisation," 2006). Besides that this technique allow the microfiber with both ends pigtailed which is very important in practical applications that have issue on connectivity("Optical fibre nanotaper sensors," 2010). In this work, the microfiber was fabricated based on a flame brushing technique using a homemade fiber tapering machine as illustrated in Figure 2.7. The fabrication rig utilizes an oxy-butane burn, micro-controller, and stepper engines.

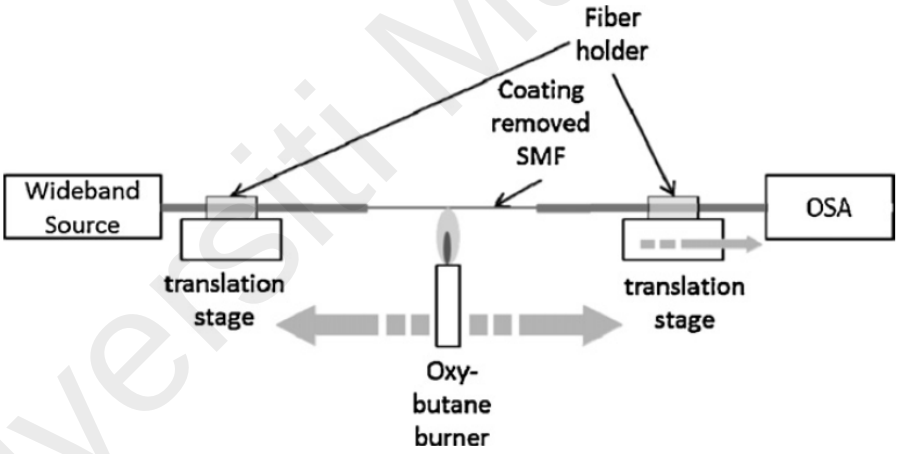

Figure 2.8: Experimental setup for flame brushing technique to produce microfiber ("Theoretical analysis and fabrication of tapered fiber," 2013)

Besides of the tapering method, heat sources also play essential role to produce a good quality microfiber. There are four heat sources have been commonly used during the tapering process such as flame("Biconical fiber taper sensors," 2006), fusion splicer("Design of humidity sensors based on tapered optical fibers," 2006), CO_2 laser beam ("Miniature all-fiber devices based on CO 2 laser microstructuring of tapered fibers," 2001) and micro furnace("Design of humidity sensors based on tapered optical

Universiti Malaya

fibers," 2006). The microfiber could be fabricated into different shapes and properties by controlling pulling conditions such as length of the heated zone, pulling temperature and pulling speed. The most common heat source is an hydrogen flame, which was applied at the centre of the fiber as shown in Figure 2.8. The fiber is stretched and elongated gradually under a certain pulling force. The heating and pulling process continues until the desired length or diameter is achieved. Both ends of the fabricated microfiber is attached to the standard fiber which also known as "biconical" fiber taper("Optical microfibers and nanofibers," 2013). The waveguides properties of the microfiber could be monitored during the pulling process in term of propagation loss, multimode interference and group velocity delay("Biconical taper coaxial coupler filter," 1985). The use of flame-heated technique has disadvantages of random turbulence of the flame and oxygen during the burning process. Thus, CO_2 laser has also been introduced to solve this issue("Optical microfibers and nanofibers," 2013). Direct laser heating provide a self-regulating control which automatically stops the stretching process when the fiber diameter reaching a desired value ("Absorption and scattering of light by small particles," 2008; "Carbon dioxide laser fabrication of fused-fiber couplers and tapers," 1999). Other technique is electrically heated taper drawing, which offer more flexibilities in drawing microfiber. This technique enables to shape the microfiber into various geometries by precisely control the temperature distribution ("Near-field characterization of glass microfibers on a low-index substrate," 2010; "Optical microfibers and nanofibers," 2013).

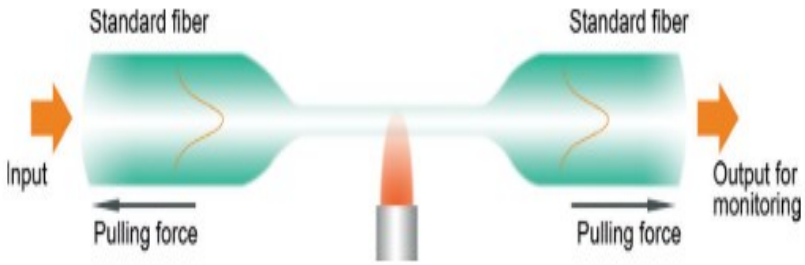

Figure 2.9: Fabrication technique of the microfiber using flame heated source (Wu & Tong, 2013)

Universiti Malaya

CHAPTER 3 : MICRO-BOTTLE RESONATOR FOR LIQUID ETHANOL SENSING

3.1 Introduction

Optical micro-resonators (OMRs) have been used in various applications in lasers, sensors and plasmonic devices (Berini, 2009; Chiasera et al., 2010). They come in various structures including micropillar, micro-ring and micro-disc that produce resonance at certain wavelengths due to continuous internal reflections in the resonators (Armani et al., 2004; Kokubun, 2005; Lee et al., 2006). The concept of internal reflections was firstly discovered by Lord Rayleigh who observed that along the dome length at some specific point, the sound could be heard clearly (Rayleigh, 1910). The sound wave was then named the whispering gallery modes (WGM). The concept was then replicated in other OMRs with similar structures to generate the WGM sound along their lengths.

Sensors based on OMRs are favourable because they are easy to fabricate, have lower losses and high quality factor (Q-factor) (Bianucci, 2016; Lee et al., 2007). One of the WGM resonators that captures the interest of researchers is the micro bottle resonator made of silica-based fiber (Bianucci, 2016; Murugan et al., 2009). It has a high Q-factor and noticeable free-spectral range. Additionally, the WGM of MBR is not perturbed by high external electromagnetic fields (Jali et al., 2018; M. Johari et al., 2018). Due to these advantages including a high sensitivity, the MBR has been used for many sensing applications including humidity and formaldehyde sensing (Johari, Khudus, Jali, Al Noman, et al., 2019; Matsko & Ilchenko, 2006b).

In this chapter, the MBR based ethanol liquid sensor is proposed and demonstrated. The MBR was constructed from a standard silica fiber, SMF28 using the "soften-and-compress" method (Murugan et al., 2011). For characterization of the MBR, a microfiber with a 3μm diameter was used with an optical power meter and a tuneable

Universiti Malaya

laser source. Then the MBR was employed for sensing liquid ethanol of 10% - 100% ppm concentration. Here, the performance of an MBR ethanol sensor was investigated and compared to that of a bare microfiber sensor.

3.2 Optical Micro-Bottle Resonator (MBR) Fabrication

The micro-bottle resonator (MBR) was fabricated using a technique known as "soften-and-compress". This technique can be used to transform a silica single mode fiber (SMF-28) into a bottle structure by crafting a bump in the midriff area. A manual splicing machine (Furukawa Electric Fitel S178A) shown in Figure 3.1 was used for this process. In the process, the silica fiber was firstly clamped on a holder and heated by the fusion mode of the splicing machine. The heat was applied to the midriff area of the fiber. As the heated area softened, it was compressed slowly inwards from both sides. This action created a bulge or bottle structure at the centre of the silica fiber, where the diameter of bottle was determined by the numbers of arc performed (Murugan et al., 2009). The size of bottle is dependent on the number of arcs applied during the MBR fabrication process. To ensure precision of the MBRs, several parameters were controlled on the splicer machine during the process. For instance, the heating time and common arc power was set to be 25 second (per heat mode) and 111, respectively. Figure 3.2 shows how the bottle size changes by increasing the number of arcs. The resulting bottle structure resonator (MBR) was defined by three parameters: bottle diameter D_b, stem diameter D_s and bottle length L_b. In this experiment, a MBR with a bottle diameter of 170 µm, a stem diameter of 125 µm and bottle length of 180µm was successfully fabricated as shown in Figure 3.3.

Universiti Malaya

Figure 3.1: A splicer machine used to fabricate MBR structure

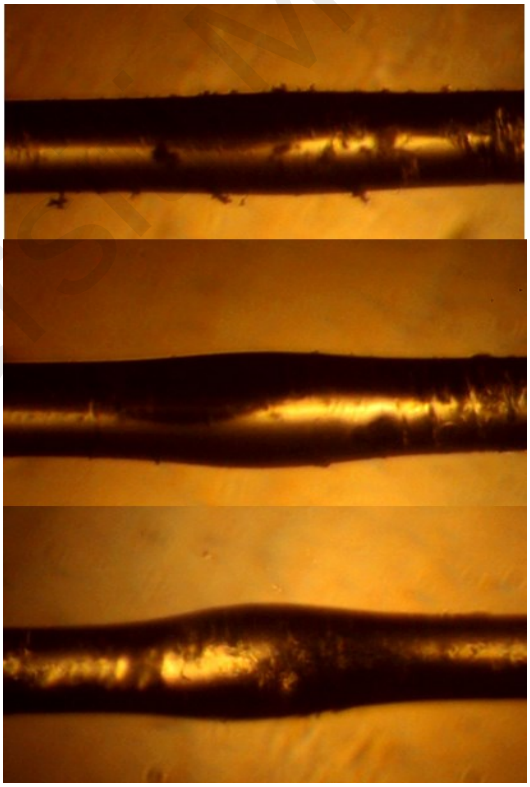

Figure 3.2: The size of 'bottle' changed by the increase of arcs numbers applied on midriff area of silica fiber to form a MBR

University Malaya

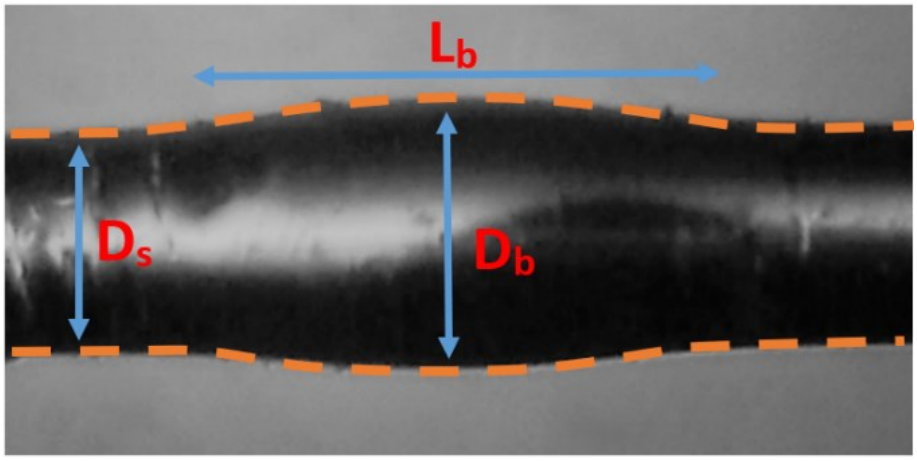

Figure 3.3: The MBR fabricated from SMF-28 with L_b = 180µm, D_b = 170µm and D_s = 125µm

3.3 Fabrication of a Microfiber

At first, a microfiber was fabricated for use in in conjunction with MBR structure for sensing using a homemade fiber tapering machine. Figure 3.4 shows the schematic diagram of the tapering machine. A sensing region was formed by mechanically stripping the buffer layer of a single-mode fiber (SMF, Corning SMF-28, USA) with a diameter of 125µm and subsequently cleaning the stripped region with alcohol solution. Then, the stripped region was placed horizontally in between two fiber holders. One of the fiber holder was placed onto a YZ translation stage. The stripped region was heated by the moveable flame produced from the oxy-butane burner. While the moving flame heat along the stripped region, the heating and pulling process was also executed spontaneously to stretch the fiber at a fix tapered length of 2cm. The tapering process was performed by controlling several elements such as flame movement, fiber stretching length and speed (Lim et al., 2012b). Figure 3.5 shows the bare microfiber sensor with a diameter waist of 3 µm, which was captured by using a microscope with 20 times magnification. It was fabricated from SMF-28 silica fiber using the “flame brushing”

Universiti Malaya

technique. The fabricated bare microfiber was first used in the characterization of the MBR and later as a sensor for performance comparison.

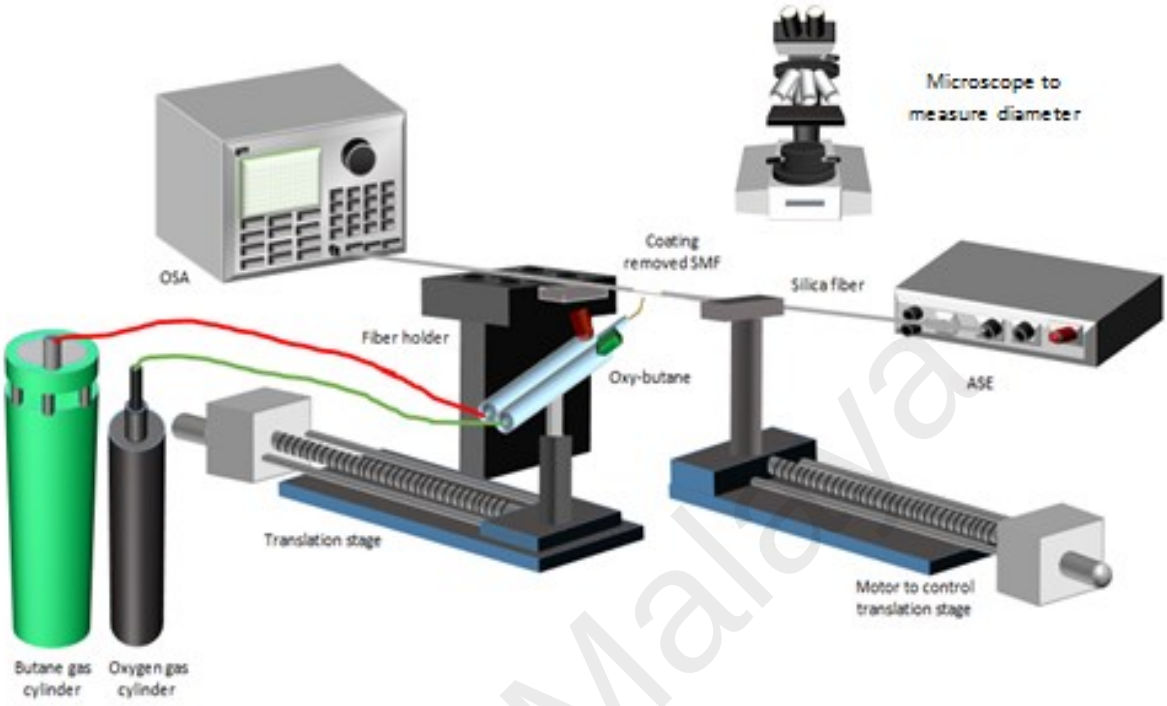

Figure 3.4: Heating and pulling process using flame brushing technique

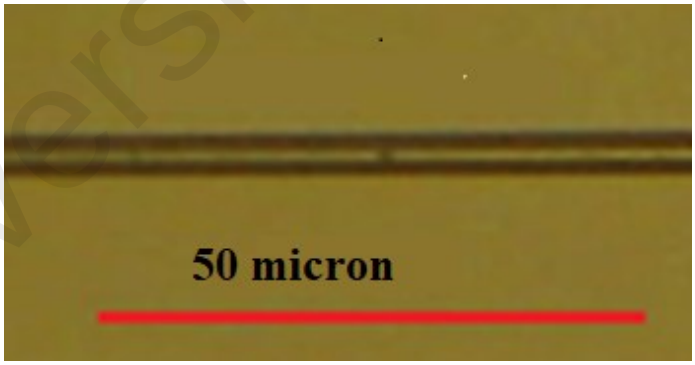

Figure 3.5: Microscopic view of a microfiber with diameter of 3 µm.

3.4 Optical MBR Characterization

In the characterization of the MBR, a tuneable laser source (ANDO AQ4321D) was used to supply a range of input wavelength to the sensor and an optical power meter (THORLABS S145C) was used to record the output power. The tuneable laser source

Universiti Malaya

(TLS) was able to supply wavelength in range between 1520 nm to 1620 nm. However, for the MBR characterization, the wavelength from the TLS was tuned from 1550 nm to 1575 nm with a 0.001 nm interval. The wavelength was launched into the MBR through the bare microfiber with a 3µm waist diameter. The final output power was detected by the optical power meter at the output end of the MBR. Figure 3.6 shows the transmission spectral of the MBR with several sharp resonant peaks (Nasir et al., 2016a). The graph suggests that the insertion loss for the MBR and microfiber is roughly about 17 dB and it could be enhanced by controlling the coupling gap between the MBR and the tapered microfiber (Cai et al., 2000). The Q-factor is used as an indicator to determine the quality of resonant peak of the MBR and it is defined as $\Delta\lambda/\lambda$ where λ is the resonant wavelength. At 1.534 x 10^5, it is smaller than the one reported in (Nasir et al., 2016b). The is because the sizes of the tapered microfiber and the MBR, hugely influence the Q-factor and insertion loss.

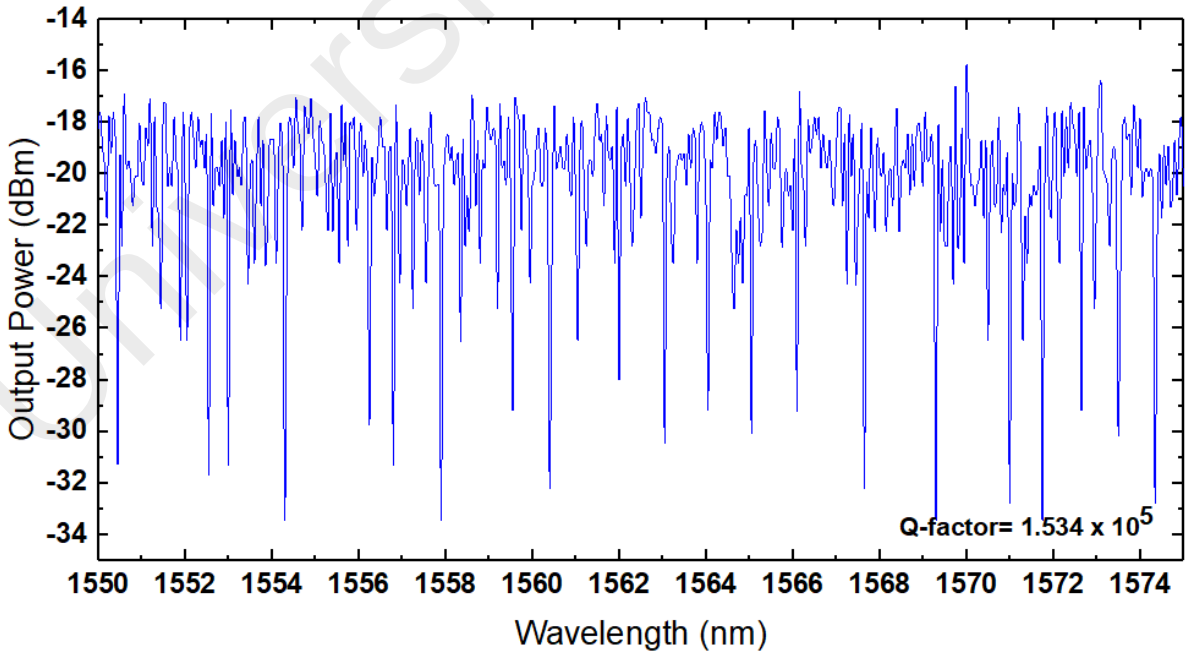

Figure 3.6: The transmission spectral of the MBR with several resonant peaks, which was obtained by launching a tuneable light source into the MBR structure via a tapered microfiber with 3 µm waist diameter.

Universiti Malaya

3.5 Experimental Procedure for the MBR as Liquid Ethanol Sensor

Ethanol an organic chemical compound with a simple structure. Figure 3.7 shows the molecular structure of ethanol, which consists of two single bonded carbon atoms with five hydrogen atoms as well as hydroxyl (OH) group moieties (Alzeer & Hadeed, 2016; Pauzi et al., 2019). It is a colourless organic liquid, which can be produced naturally from fermentation of plant or synthesized from petroleum by product.

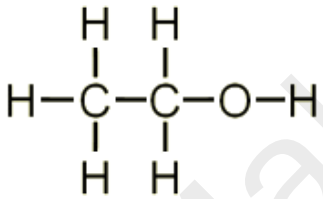

Figure 3.7: Structure of ethanol molecule

Ethanol concentration is an important parameter often measured in research, food and beverage processing. The accurate amount of ethanol percentage in food and beverage is crucial to ensure the safety and quality of products. Excessive consumption of ethanol may lead to alcohol intoxication, short term memory loss, anxiolytic effect, locomotor suppression, loss of righting reflex and death (Pauzi et al., 2019). Therefore, various ethanol sensors based on different sensing principles have been reported and they include surface acoustic wave (Giffney et al., 2011), electric field (Roshan & Sheikhi, 2020) and fiber-optic (Hernaez et al., 2018). Fiber optic sensors offer many advantages such as compactness, high sensitivity, and electromagnetic interference immunity. For instance, a zinc oxide, ZnO nanorod coated long-period grating was reported for ethanol vapor sensing (Konstantaki et al., 2012). In this work, an MBR based optical fiber sensor is proposed for measuring liquid ethanol concentration. First, a few liquid ethanol concentrations were prepared by mixing ethanol with distilled water as shown in Figure

Universiti Malaya

3.8. Then an experiment was conducted to test the ability of the MBR and bare microfiber sensors to detect the various liquid ethanol concentrations.

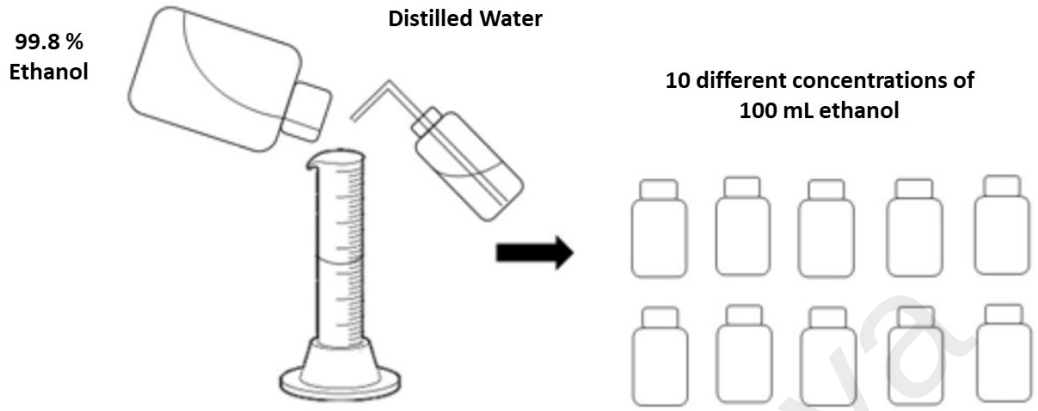

Figure 3.8: Preparation of liquid ethanol (EtOH) of different concentrations.

The experimental setup is shown in Figure 3.9. The MBR coupled to a bare microfiber sensor is fixed by the stage with an ethanol liquid placed on the bottom of the stage. The MBR is positioned between the microfiber and liquid ethanol. This is to ensure the MBR was able to couple with the microfiber and touch the ethanol at the same time. The sensor and ethanol were sealed inside a chamber at ambient room temperature of 25^0C and atmospheric pressure of 1.0 atm. One end of fiber was connected to TLS while another end was connected to the OPM. The output power was recorded for different ethanol concentration, which varied from 10% to 100%. Since the MBR resonance was obtained at 1558 nm, the TLS wavelength was fixed at 1558 nm during the measurement. To minimize random error and analyse the repeatability of the ethanol liquid sensor, the experiment was repeated three times. The stability of the sensor is determined by recording the output in a period of 20 minutes interval at different ethanol concentrations. The experiment was also replicated by replacing the MBR with a bare microfiber (no-MBR used) for comparison purpose.

Universiti Malaya

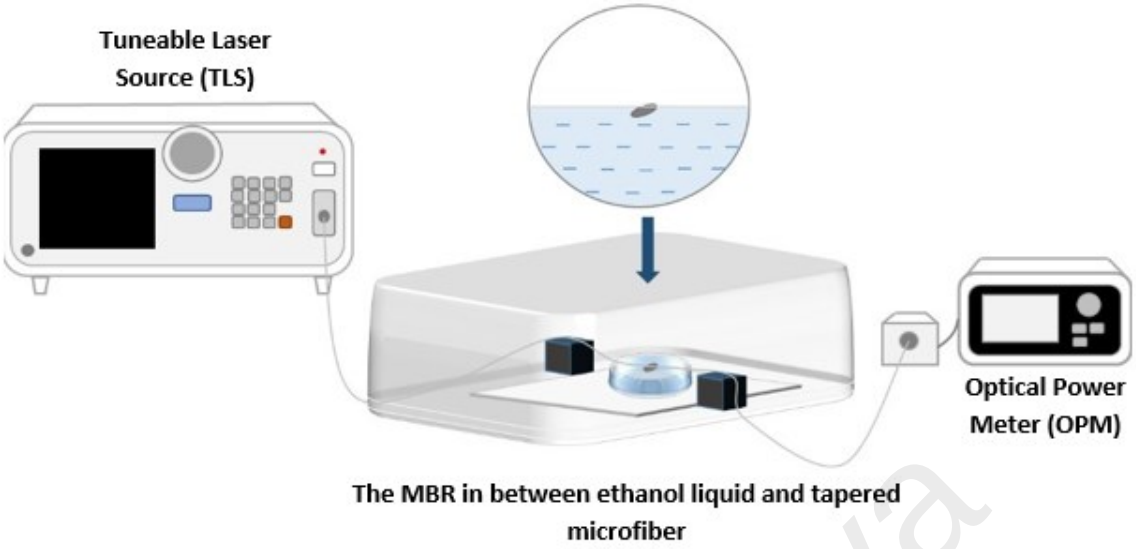

Figure 3.9: The experimental setup where the MBR or bare microfiber sensor was placed in the ethanol liquid.

3.6 The MBR and Bare Microfiber Performance as Liquid Ethanol Sensor

The averaged output power (dBm) of the MBR and bare microfiber (no-MBR) at different concentrations of ethanol are shown in Figure 3.10. Generally, the output power increases with the level of ethanol concentration for both experimental conditions, with and without the MBR in the setup. Table 1 summarizes the performance of the sensors in terms of sensitivity, linearity, and standard deviation. It is obvious that the MBR performs better than the bare microfiber (no-MBR used) in all aspects. The sensitivity of the MBR at 0.1756 dB/%.ppm, is much higher than that of the bare microfiber at 0.1049 dB/%.ppm. The linearity of the MBR is 99.28% as opposed to that of the bare microfiber, which is only 83.01%. These results indicate that the MBR outperforms the bare microfiber as an ethanol liquid sensor. This is because the total surface and consequently the surface absorption of the MBR is higher. Therefore, light was circulated multiple times as it passes through the MBR structure. Each passes increases the adsorption, thus increasing the sensitivity (Arregui et al., 1999; Batumalay et al., 2015).

Universiti Malaya

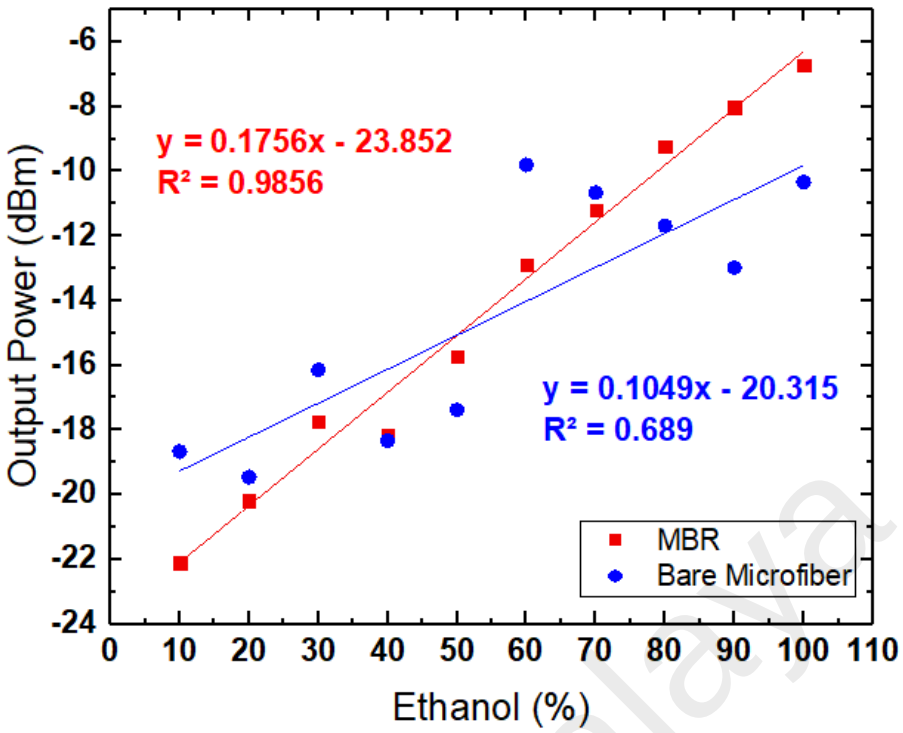

Figure 3.10: The output power against ethanol concentration for MBR and bare microfiber sensors.

Table 3.1: Performance of bare microfiber and MBR sensors for ethanol liquid concentration measurement

Parameters	**Bare Microfiber**	**With MBR**
Linearity (%)	83.01%	99.28%
Sensitivity (%)	0.1049	0.1756
Standard deviation (dBm)	5.827	3.355
Linear Range (%)	10 - 100	10 - 100

.

The same experiment was performed three times for both sensors, MBR and bare microfiber, to study the repeatability of the results (Isa et al., 2018). Figures 3.11 (a) and (b) display the results of the three cycles of experiment for the MBR and the bare microfiber sensor, respectively. The MBR's sensitivity is always more than 0.16

Universiti Malaya

dB/%ppm while bare microfiber's sensitivity is less than 0.11 dB/%ppm. The MBR sensor also scores a higher linearity with less fluctuation.

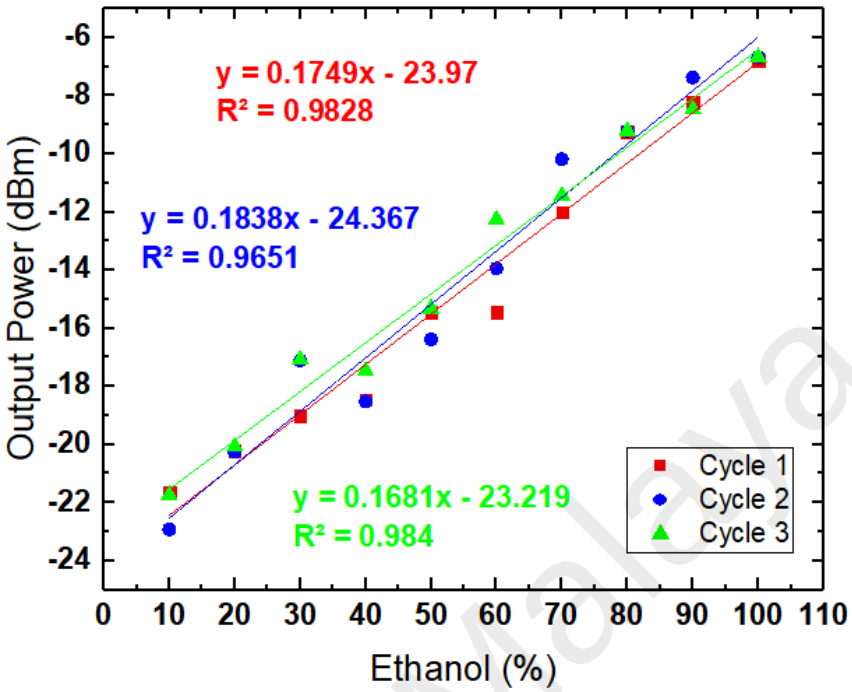

(a)

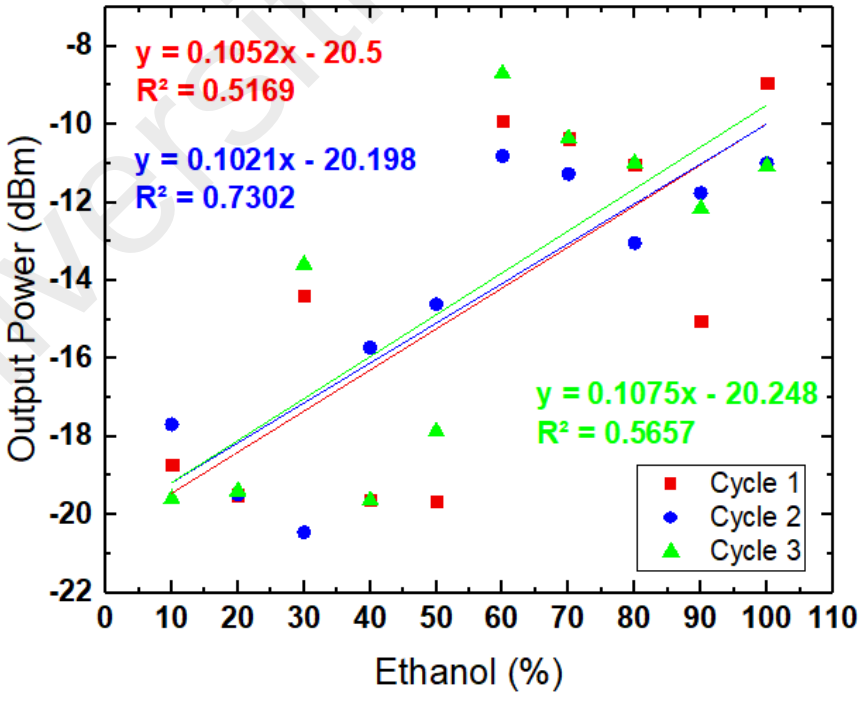

(b)

Figure 3.11: Repeatability performance of (a) MBR and (b) bare microfiber varies with different ethanol concentrations

Universiti Malaya

The stability of the MBR and bare microfiber sensors were recorded for a period of 20 minutes as shown in Figures 3.12 (a) and (b), respectively. As seen, both sensors are remarkably stable during the observation. Even though the test period is quite long, both the MBR and bare microfiber sensors readings are not interrupted by other noises. Thus, both the MBR and bare microfiber are sufficiently stable to be used as ethanol liquid sensors (Isa et al., 2018).

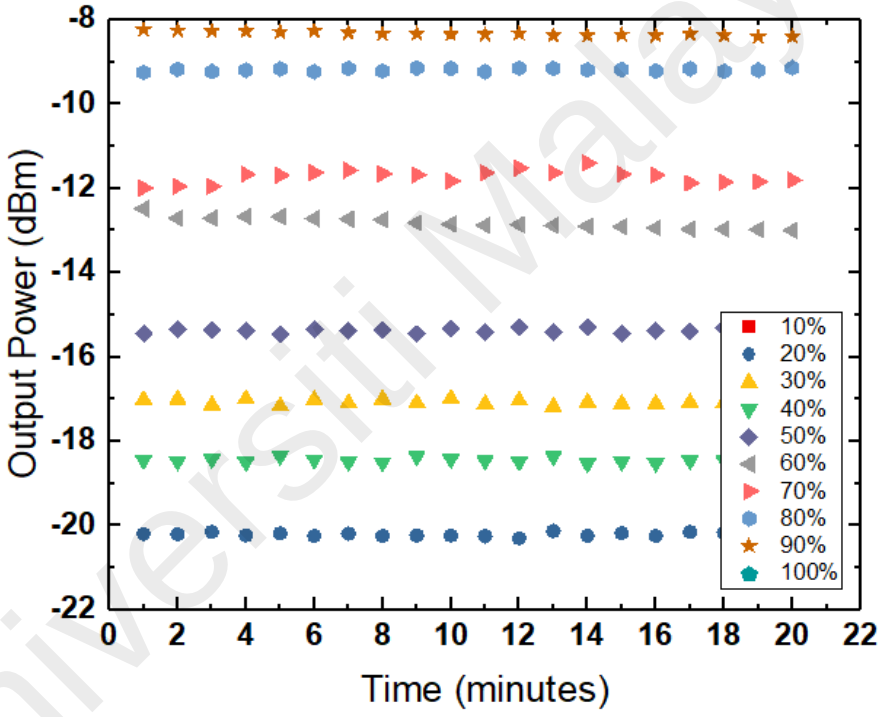

(a)

Universiti Malaya

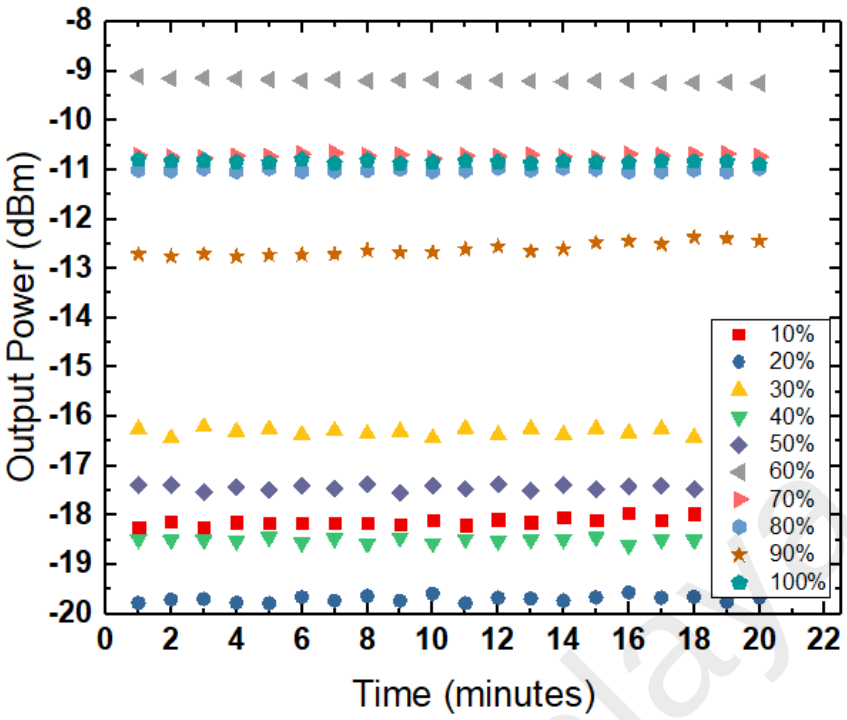

(b)

Figure 3.12: Stability performance of (a) MBR and (b) bare microfiber for each ethanol concentrations varies with time

Figures 3.13 (a) and (b) show the transmission spectra at various ethanol concentrations for the MBR and bare microfiber sensor, respectively. As seen in Figure 9(a), the resonance wavelength of the MBR shifts to a longer region from 1561 nm to 1567 nm as the ethanol concentration was increased from 10% to 100%. This is attributed to the increase of the surrounding refractive index with the increase of the ethanol concentration which reduces the refractive index contrast of the MBR structure. This increases the transmission loss and forces the resonance wavelength to shift to the longer wavelength, which has a lower loss. On the other hand, the transmission spectrum of the bare microfiber broadens as the ethanol concentration increases. This causes a slightly shift in the centre wavelength from 1560 nm to 1562 nm as the ethanol concentration increases from 10% to 100%. In short, the bare microfiber is less sensitive to ethanol

Universiti Malaya

concentration change than the MBR. Therefore, the MBR works better than the bare microfiber as a liquid ethanol sensor.

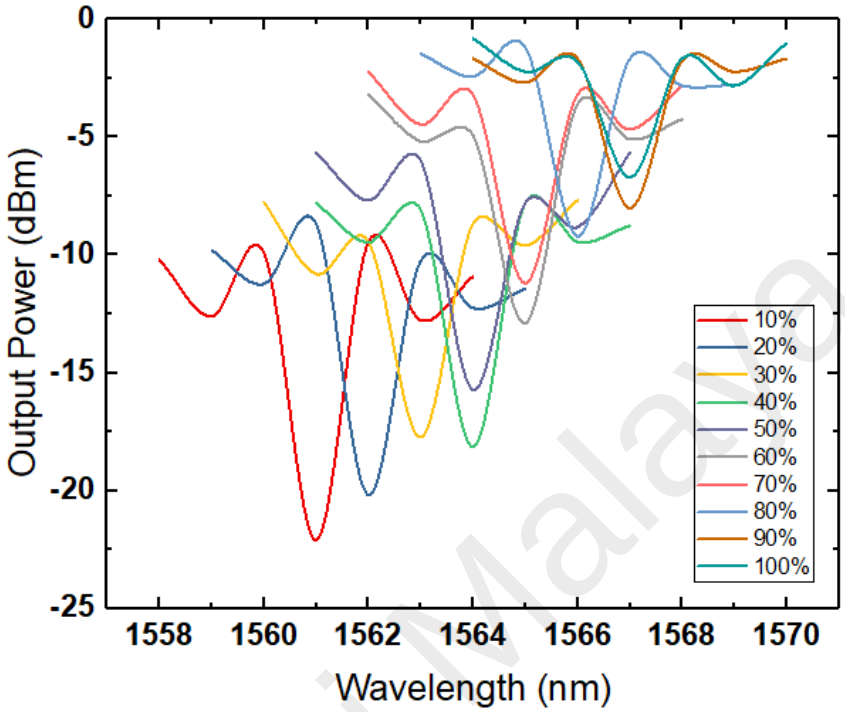

(a)

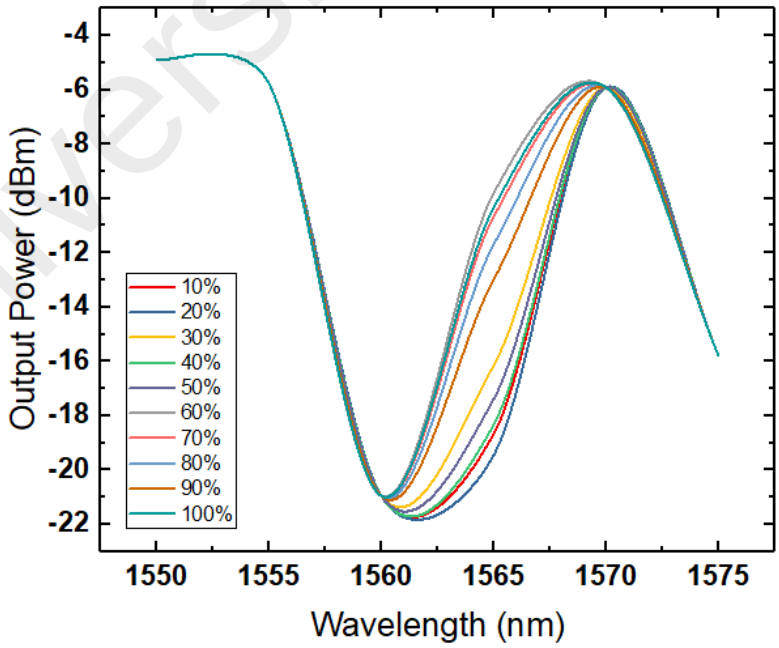

(b)

Figure 3.13: Wavelength shift of (a) MBR and (b) bare microfiber on every liquid ethanol concentration

Universiti Malaya

3.7 Summary

The liquid ethanol sensing was successfully demonstrated using the MBR structure as a probe. It performs better than the conventional probe with only a bare microfiber. The proposed MBR sensor has a sensitivity of 0.1756 dB/%ppm, linearity of 99.28% and a standard deviation of 3.355 dB. The sensor was also found to have a good stability as it was tested about 20 minutes for three times. The MBR's resonance wavelength was shifted by around 6nm as the ethanol concentration was increased from 10% to 100%.

Universiti Malaya

CHAPTER 4 : MICRO-BOTTLE RESONATOR FOR SODIUM HYPOCHLORITE SENSING

4.1 Introduction

Sodium hypochlorite, NaOCl, solution, is one of the industrial chemicals, which has been widely employed for cleaning application. This is attributed to its properties as a good disinfectant. While NaOCl is an outstanding cleaning solution, at high concentrations it can harm the environment and damage drainage pipes. Therefore, it is important to remotely monitor the concentration of sodium hypochlorite within sealed pipes so that the environmental integrity can be ensured. If unnecessary quantities of NaOCl are found, appropriate measures can be taken to neutralize the chemical. On the other hand, optical micro-resonators (OMRs) have gained significant interest in recent years due to its extensive applications in optical sensor and laser (Ahmad et al., 2019; Md Ashadi et al., 2019; Tian et al., 2020).

Various structures such as micro-disks, micro-pillars and micro-rings have been proposed and used to confine and store light for a period of time by total internal reflections (Anguiano et al., 2017; Srinivasan & Painter, 2007; Zhang et al., 2019). Resonant modes can be realized inside the cavity if the confined light is in phase with itself after one round trip. These resonant modes are referred to whispering gallery modes (WGMs). WGM resonators have been intensively studied due to its notable advantages including simplicity of fabrication, high Q-factors and low intrinsic losses (Bianucci, 2016; Lee et al., 2007). The micro-bottle resonator (MBR) is one subclass of WGM resonators, has recently gained popularity due to its capability to achieve high Q factor and free-spectral range especially for silica based resonators (Bianucci, 2016; Murugan et al., 2009). These parameters are important for various sensing applications.

Universiti Malaya

In this chapter, MBR sensor is proposed and demonstrated for measuring hypochlorite concentration in water. The MBR used was fabricated by using a method known as "soften-and-compress" from a standard silica fiber (SMF-28). A 2µm microfiber was used to launch a light into MBR for the sensing different liquid sodium hypochlorite with various concentrations ranging from 1% – 6% ppm. The MBR sensor performance was then compared with bare microfiber based sensor (Kronenberg et al., 2002; Xu et al., 2004).

4.2 Experimental Arrangement

The MBR in this research was fabricated from a standard single mode fiber (SMF-28) using a fusion splicer based on a "softened-and-compress" technique (Murugan et al., 2011). The fusion splicer operates based on a thermo-mechanical process in which the cleaved ends of two optical fibers are pushed towards each other during the arcing. During this process, they are heated to a high temperature at which both cleaved fibers are soften and fuse together. This splicing action was exploited on a piece of continuous fiber in this experiment to soften a small region of the fiber while simultaneously compressing it. The SMF-28 silica fiber was manually fixed in a manual splicing machine (Furukawa Electric Fitel S178A). The middle area of the fiber was heated at its softening point by arc discharge to create constriction. This step was repeated in another location so that the heated area can be compressed inward direction, resulting in the creation of bulge structure in the optical fiber. We used multiple short arcs with arc duration of about one second to controllably soften the SMF-28. This procedure results in a robust MBR with the bottle diameter D_b, the stem diameter D_s and the neck-to-neck length L_b of 180 µm, 125 µm and 183 µm respectively, as shown in Figure 4.1. The shape of the bulge is defined by the softening temperature profile and the applied compression. On the other

Universiti Malaya

hand, a tapered microfiber was fabricated from the similar SMF-28 using a "flame brushing" technique using silica fiber SMF-28 (Lim et al., 2012b).

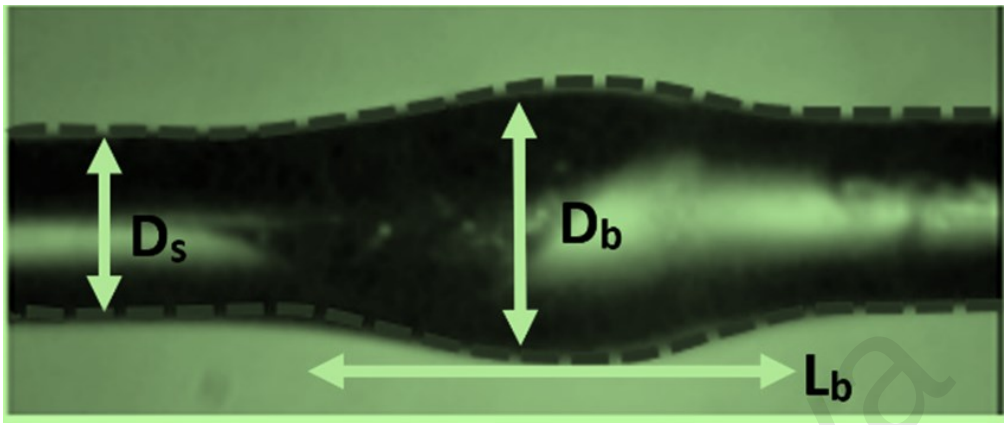

Figure 4.1: The MBR fabricated with L_b = 183 μm, D_b = 180 μm and D_s = 125 μm

The characterization of the MBR was carried out by using tuneable laser source (ANDO AQ4321D) in conjunction with an optical power meter (THORLABS S145C). The tuneable light was launched into the MBR via a tapered microfiber with 2 μm thickness diameter. In the experiment, the laser was tuned from 1552.00 nm to 1552.30 nm with 0.001nm wavelength interval while the output power was collected by the same microfiber and measured by an optical power meter. Figure 4.2 shows the transmission spectrum from the MBR structure, which indicates several sharp resonant depths of WGMs. The MBR combines WGMs with "bouncing ball" modes, featuring caustics that restrict the propagation about the axial direction, with a Q-factor on the order of 105. The insertion loss of the MBR structure is observed to be around 17 dB. The high loss was obtained due to coupling gap between the MBR the tapered microfiber. However, it can be controlled with the proper handling during the coupling procedure (Cai et al., 2000). The Q-factor is defined by $\lambda/\Delta\lambda$ where λ is the resonant wavelength and it represents the quality standard reached by the MBR. The Q-factor to the fabricated MBR is approximately 7.95 x 105 which is similar to the previous works (Johari et al., 2020). This is thought to happen due to the insertion loss of the entire MBR ensemble.

Universiti Malaya

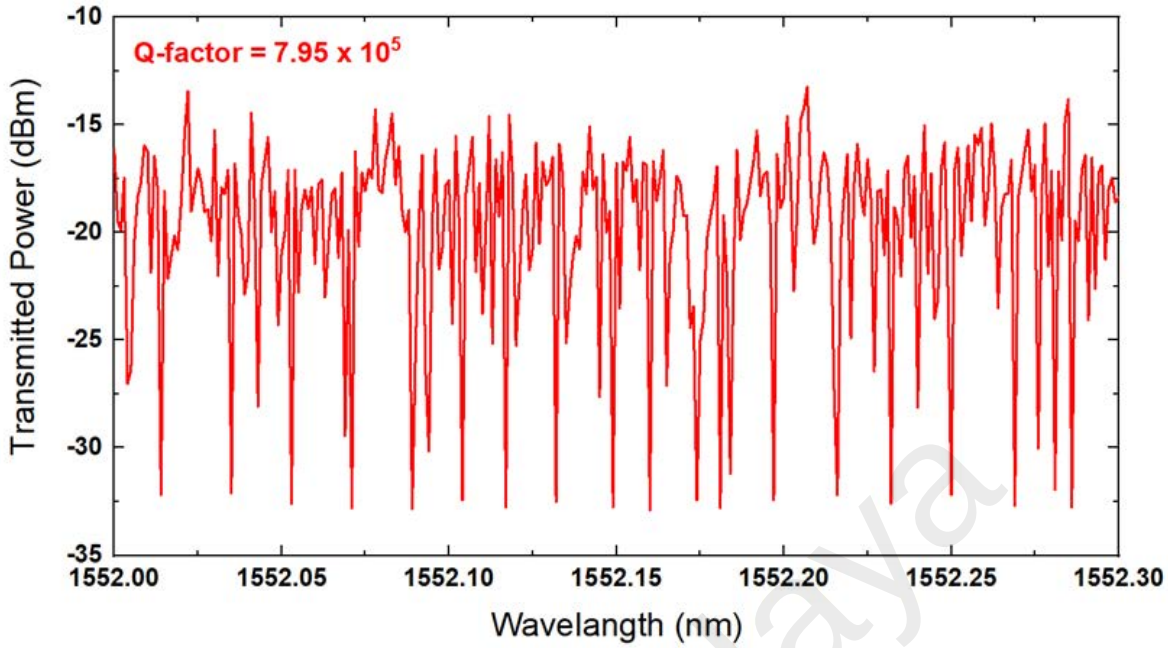

Figure 4.2: Transmission spectral characteristic of the MBR

MBRs have not been used significantly as sensing devices where the medium to be analysed lies outside the resonator. Here, the MBR was used to measure a sodium hypochlorite concentration in water and the experimental setup is shown in Figure 4.3. The MBR structure coupled with tapered microfiber was used as a sensor probe and it was placed inside a sealed chamber to control humidity and temperature during the experiment. The room temperature and humidity were set at 25^0C and 40 % RH; where monitored by the temperature sensor and hygrometer (RS 1365). One end of the microfiber connected to the tuneable laser source while another end is connected to optical power meter. Tuneable laser source operating at a resonance wavelength of the MBR was used as a light source and the output power was recorded by the optical power meter. The concentration of the sodium hypochlorite liquid was then varied from 1 % ppm to 6 % ppm during the measurement. At first, the wavelength was set at 1552.15 nm and the output power for different concentration of sodium hypochlorite was recorded. To minimize random error, the experiment was carried out by three times. The MBR was then replaced by bare microfiber for sodium hypochlorite sensing for comparison

Universiti Malaya

purpose. To ensure stability of the sensor, the transmission output power was also recorded within 120 minutes duration at 6% ppm of concentration level. The transmission spectral characteristics of the MBR was also investigated at various sodium hypochlorite concentrations. The bottle WGM resonances were observed by sweeping the wavelength of light source.

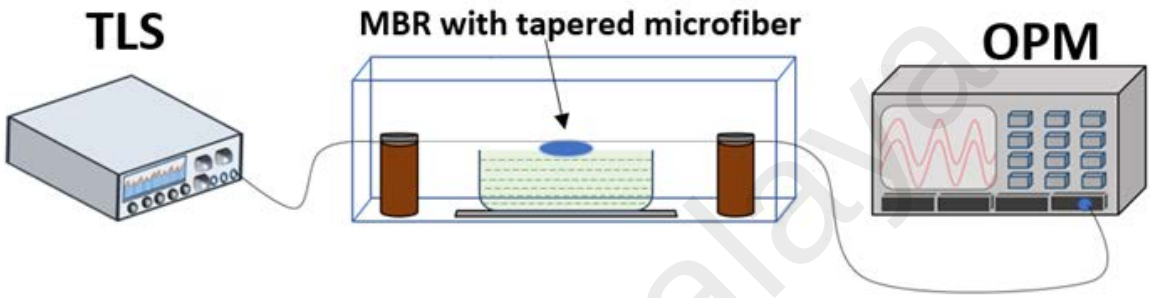

Figure 4.3: Experimental setup for sodium hypochlorite concentration sensor.

4.3 Sensing Performance

During the output power characterization, it was observed that the transmitted power level was varied with the variation of sodium hypochlorite concentration for both MBR and no-MBR microfiber-based sensors. In Figure 4.4, we plot the variation of the transmission power, corresponding to sodium hypochlorite concentrations. It is observed that the transmission power decreased by the increasing of concentration percentage for both sensors. However, the sensing sensitivity was significantly improved using MBR. As recorded, the sensitivity of the MBR sensor is 3.7319 dB/%ppm while bare microfiber sensor managed to exhibit only 0.7176 dB/%ppm sensitivity. Same goes with the linearity were the MBR sensor exhibit 92% linearity, which is significantly higher that bare microfiber-based sensor (64%). This indicates that the WGMs inside the MBR plays an important role in improving the sensor sensitivity. This is attributed to the refractive index

Universiti Malaya

of the sodium hypochlorite liquid, which increase with the concentration and thus slightly shift the resonance wavelength (Jali et al., 2019; M. A. M. Johari et al., 2018; Johari, Khudus, Jali, Maslinda, et al., 2019; Yusof et al., 2019). The wavelength shift increases the loss inside the MBR and reduces the transmission power as observed in Figure 4.4.

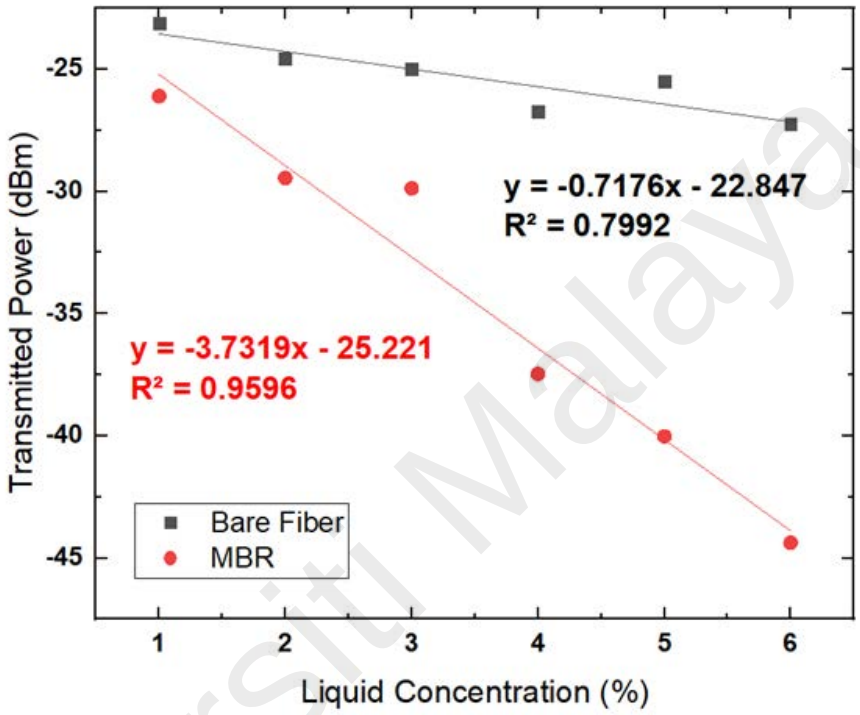

Figure 4.4: The transmitted power against sodium hypochlorite concentration for MBR and bare microfiber sensors.

Another method for detecting changes of sodium hypochlorite concentration is by measuring resonance shifts as shown in Figure 4.5 (a). This figure shows that the WGM's resonance wavelength shifted from 1552.203 nm to 1552.213 nm as the concentration increased from 1% to 6%. This wavelength shift is attributed to the change in the refractive index of the surrounding liquid. Figure 4.5(b) shows the relation between the resonance wavelength against the sodium hypochlorite concentration. It is shown that the MBR based sensor has a sensitivity of 0.002 nm/%ppm with linearity of 97.64%. The relatively low linearity is due to the resonance shifts, which are also subject to noise from

Universiti Malaya

the laser or temperature fluctuations. The linearity can be improved by careful control of the resonator environment to mitigate the noise.

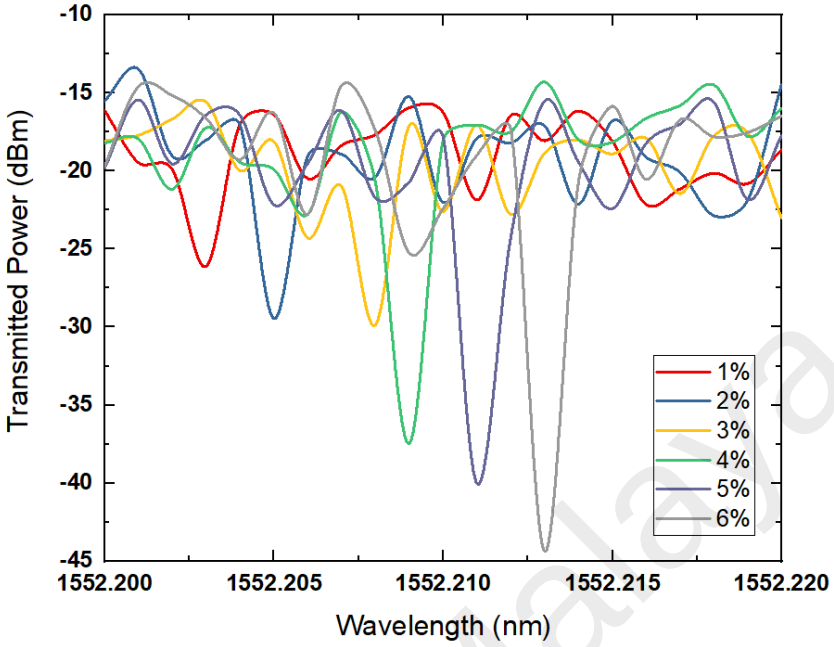

(a)

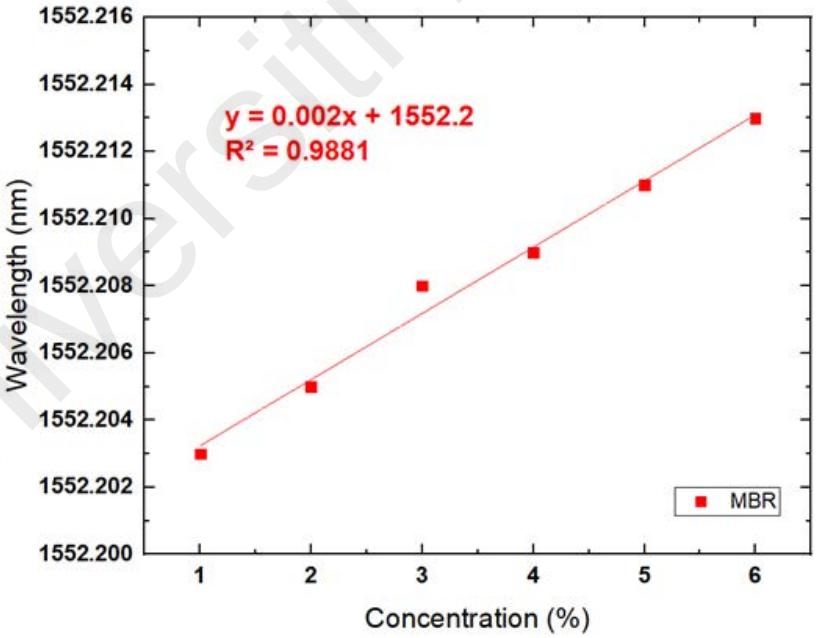

(b)

Figure 4.5: WGM's resonance wavelength shift result (a) Transmission spectral at various concentration level (b) Resonance wavelength against the concentration.

Universiti Malaya

Figure 4.6 presents the transmitted power stability from the proposed MBR and bare microfiber sensors, for a duration of 120 minutes when the sodium hypochlorite concentration is fixed at 6%. Both the MBR and bare microfiber sensors were observed to stably perform during this time duration. The output power fluctuation is noticed to be lower than 5% for both sensors. It is observed that the coupling between the MBR structure and tapered microfiber is quite durable if no perturbations was applied to the setup. However, permanent coupling should be studied and employed for practical use of the sensor.

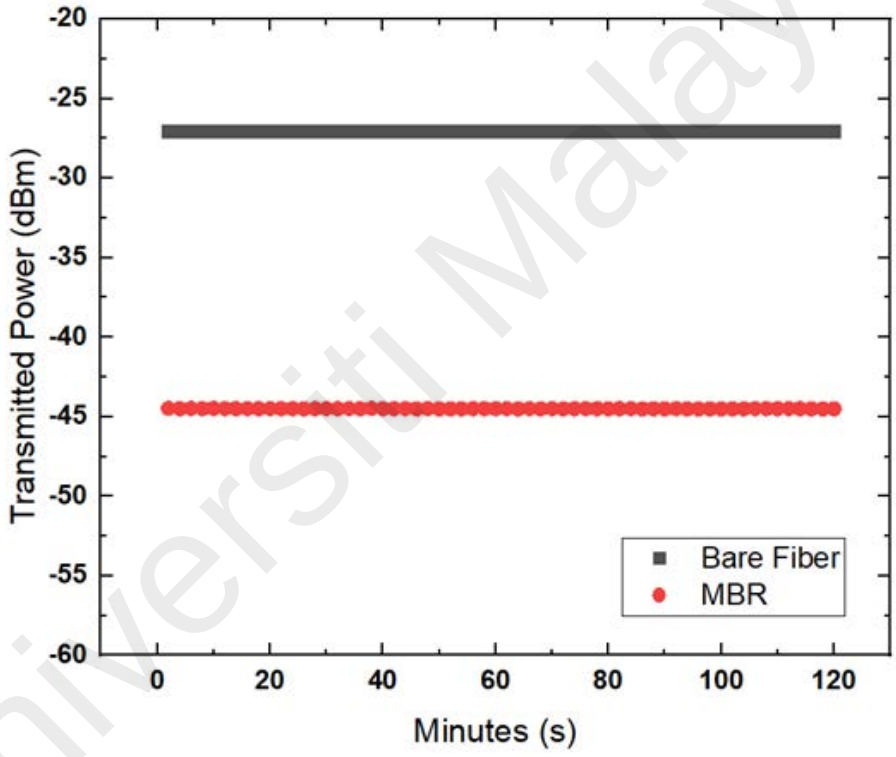

Figure 4.6: The transmitted power from the MBR against time for assessing stability

Universiti Malaya

4.4 Summary

The use of a whispering gallery mode (WGM) in optical micro-bottle resonator (MBR) was successfully investigated for sodium hypochlorite sensor. The MBR was prepared by using a simple approach based on the "soften-and-compress" method. We have successfully created a bulge structure with a diameter and length of 180 μm and 183 μm, respectively. The MBR was optically excited by using a 2μm tapered microfiber and

was found to have a Q-factor of approximately 7.95 x 10^5. The MBR was then employed to measure sodium hypochlorite concentration within 1% to 6% range based on the changes in transmitted optical power and resonance wavelength. The transmitted power reduced with the increase concentration with a sensitivity of 3.7319 dB/%ppm which was superior to the bare microfiber. The MBR sensor was also found to have a linear resonance wavelength shift against the concentration with a sensitivity of 0.002 nm/%ppm. This indicates that MBR sensor has a huge potential to be utilized as a low-cost sodium hypochlorite sensor.

Universiti Malaya

CHAPTER 5 : CONCLUSION AND FUTURE WORK

Optical whispering gallery mode (WGM) micro-resonators, confining resonant photons in a microscale resonator for long periods of time, could strongly enhance light-matter interaction, making it an ideal platform for all kinds of sensors. For instance, optical micro-bottle resonator (MBR) structure fabricated based on arc fusion approach was widely deployed to implement highly compact, low cost and versatile sensor device. This research work aimed to explore WGMs in optical MBR for sensing applications. The MBR was successfully fabricated from a silica single mode fiber (SMF-28) by using a new method known as "soften-and-compress".

At first, an optical MBR was successfully investigated for liquid ethanol sensing. The resonator was made of an SMF-28 silica fiber using a new method known as "soften-and-compress" to create a bottle structure which looks like a bump. It has a midriff diameter D_b = 170 μm, stem diameter D_s = 125 μm and bottle length L_b = 180 μm. The MBR was characterized by injecting a tuneable wavelength light source through a 3μm bare microfiber and it exhibits a quality factor (Q-factor value) of > 10^4. The fabricated MBR was then used as a liquid sensor to detect ethanol concentration within a range from 10% to 100%. The shift in the MBR's resonant wavelength was around 6nm as the ethanol concentration was increased from 10% to 100%. Its performance was compared with a bare microfiber (no-MBR) based sensor. It was found that the MBR ethanol liquid sensor showed a sensitivity of 0.1756 dB/%ppm, linearity of 99.28% and standard deviation of 3.355 dB, which were significantly better than those of the bare microfiber sensor. The sensor maintained a good stability while in operation for over 20 minutes and it remained stable when the experiment was repeated three times.

The MBR based sensor was also proposed and demonstrated for measuring sodium hypochlorite concentration. The MBR with a bottle diameter (D_b), bottle length

Universiti Malaya

(L_b) and stem diameter (D_s) of 180 μm, 183μm and 125 μm respectively, was successfully fabricated based on a "soften-and-compress" method utilizing a fusion splicer. We used a tapered microfiber with a 2μm diameter to launch light into the structure and the wavelength gallery modes resonances are observed with a Q-factor approximately 7.95×10^5. It is obtained that transmitted light power from the MBR reduces with the increase of sodium hypochlorite from 1% to 6%. The sensor sensitivity was about 3.7319 dB/%ppm, which is higher than the bare microfiber-based sensor. The whispering gallery modes resonance wavelength also shifted from 1552.203 nm to 1552.213 nm with a sensitivity of 0.02 nm/%ppm and linearity of 97.64% as the concentration increased from 1% to 6%.

These results indicates that the MBR structure has a great potential for use as a sensor. The structure of this resonator allowed it to be a good sensor, especially for liquid ethanol sensing and sodium hypochlorite sensing. This may open a new path of MBR to be applied for another type of sensing purpose in future. Both ethanol and sodium hypochlorite were in liquid medium. Based on the sensing performance in this dissertation, it is found that liquid medium could cooperate with the MBR very well. The concept of WGMs increases the sensitivity of MBR in liquid medium sensor. However, MBR was not tested for gas and solid medium. In the future, this would be a good research path for MBR sensor.

Universiti Malaya

REFERENCE

Absorption and scattering of light by small particles. (2008).

Ahmad, A., Cheng, X. S., Paul, M. C., Dhar, A., Das, S., Ahmad, H., & Harun, S. W. (2019). Self-generating Brillouin fiber laser using highly nonlinear hafnium bismuth erbium-doped fiber. *Microwave and Optical Technology Letters*, *61*(6), 1651-1655.

Almeida, V. R., Barrios, C. A., Panepucci, R. R., & Lipson, M. (2004). All-optical control of light on a silicon chip. *Nature*, *431*(7012), 1081-1084.

Alzeer, J., & Hadeed, K. A. (2016). Ethanol and its Halal status in food industries. *Trends in Food Science & Technology*, *58*, 14-20.

Anguiano, S., Bruchhausen, A. E., Jusserand, B., Favero, I., Lamberti, F., Lanco, L., Sagnes, I., Lemaître, A., Lanzillotti-Kimura, N. D., & Senellart, P. (2017). Micropillar resonators for optomechanics in the extremely high 19–95-GHz frequency range. *Physical Review Letters*, *118*(26), 263901.

Armani, A. M., Kulkarni, R. P., Fraser, S. E., Flagan, R. C., & Vahala, K. J. (2007). Label-free, single-molecule detection with optical microcavities. *science*, *317*(5839), 783-787.

Armani, D., Kippenberg, T., Spillane, S., & Vahala, K. (2003). Ultra-high-Q toroid microcavity on a chip. *Nature*, *421*(6926), 925-928.

Armani, D., Min, B., Martin, A., & Vahala, K. J. (2004). Electrical thermo-optic tuning of ultrahigh-Q microtoroid resonators. *Applied physics letters*, *85*(22), 5439-5441.

Arregui, F. J., Liu, Y., Matias, I. R., & Claus, R. O. (1999). Optical fiber humidity sensor using a nano Fabry–Perot cavity formed by the ionic self-assembly method. *Sensors and Actuators B: Chemical*, *59*(1), 54-59.

Batumalay, M., Harun, S. W., Irawati, N., Ahmad, H., & Arof, H. (2015). A study of relative humidity fiber-optic sensors. *IEEE Sensors Journal*, *15*(3), 1945-1950.

Berini, P. (2009). Long-range surface plasmon polaritons. *Advances in optics and photonics*, *1*(3), 484-588.

Universiti Malaya

Bianucci, P. (2016). Optical microbottle resonators for sensing. *Sensors*, *16*(11), 1841.

Bianucci, P., Wang, X., Veinot, J., & Meldrum, A. (2010). Silicon nanocrystals on bottle resonators: Mode structure, loss mechanisms and emission dynamics. *Optics express*, *18*(8), 8466-8481.

Biconical fiber taper sensors. (2006). *IEEE Photonics Technology Letters*, *18*(21), 2239-2241.

Biconical taper coaxial coupler filter. (1985). *Electronics Letters*, *21*(22), 1033-1034.

Birks, T. A., & Li, Y. W. (1992). The shape of fiber tapers. *Journal of lightwave technology*, *10*(4), 432-438.

Bobb, L. C., Shankar, P., & Krumboltz, H. D. (1990). Bending effects in biconically tapered single-mode fibers. *Journal of lightwave technology*, *8*(7), 1084-1090.

Brambilla, G. (2010a). Optical fibre nanotaper sensors. *Optical Fiber Technology*, *16*(6), 331-342.

Brambilla, G. (2010b). Optical fibre nanowires and microwires: a review. *Journal of Optics*, *12*(4), 043001.

Cai, M., Painter, O., & Vahala, K. J. (2000). Observation of critical coupling in a fiber taper to a silica-microsphere whispering-gallery mode system. *Physical review letters*, *85*(1), 74.

Carbon dioxide laser fabrication of fused-fiber couplers and tapers. (1999). *Applied Optics*, *38*(33), 6845-6848.

Chao, C.-Y., & Guo, L. J. (2006). Design and optimization of microring resonators in biochemical sensing applications. *Journal of lightwave technology*, *24*(3), 1395-1402.

Chen, G. Y., Ding, M., Newson, T., & Brambilla, G. (2013). A review of microfiber and nanofiber based optical sensors. *The Open Optics Journal*, *7*(1).

Chiasera, A., Dumeige, Y., Feron, P., Ferrari, M., Jestin, Y., Nunzi Conti, G., Pelli, S., Soria, S., & Righini, G. C. (2010). Spherical whispering-gallery-mode microresonators. *Laser & Photonics Reviews*, *4*(3), 457-482.

Universiti Malaya

Chu, S., Pan, W., Kaneko, T., Kokubun, Y., Little, B., Ripin, D., & Ippen, E. (1999). Fabrication of vertically coupled glass microring resonator channel dropping filters. OFC/IOOC. Technical Digest. Optical Fiber Communication Conference, 1999, and the International Conference on Integrated Optics and Optical Fiber Communication,

Chu, S. T., Little, B. E., Pan, W., Kaneko, T., Sato, S., & Kokubun, Y. (1999). An eight-channel add-drop filter using vertically coupled microring resonators over a cross grid. *IEEE Photonics Technology Letters*, *11*(6), 691-693.

Del'Haye, P., Schliesser, A., Arcizet, O., Wilken, T., Holzwarth, R., & Kippenberg, T. J. (2007). Optical frequency comb generation from a monolithic microresonator. *Nature*, *450*(7173), 1214-1217.

Design of humidity sensors based on tapered optical fibers. (2006). *Journal of Lightwave Technology*, *24*(11), 4329-4336.

Ding, L., Belacel, C., Ducci, S., Leo, G., & Favero, I. (2010). Ultralow loss single-mode silica tapers manufactured by a microheater. *Applied optics*, *49*(13), 2441-2445.

Ding, M., Senthil Murugan, G., Brambilla, G., & Zervas, M. N. (2012). Whispering gallery mode selection in optical bottle microresonators. *Applied Physics Letters*, *100*(8), 081108.

Ding, Y., Yang, Q., Guo, X., Wang, S., Gu, F., Fu, J., Wan, Q., Cheng, J., & Tong, L. (2009). Nanowires/microfiber hybrid structure multicolor laser. *Optics express*, *17*(24), 21813-21818.

Djordjev, K., Choi, S.-J., Choi, S.-J., & Dapkus, R. (2002). Microdisk tunable resonant filters and switches. *IEEE Photonics Technology Letters*, *14*(6), 828-830.

Eryürek, M., Tasdemir, Z., Karadag, Y., Anand, S., Kilinc, N., Alaca, B. E., & Kiraz, A. (2017). Integrated humidity sensor based on SU-8 polymer microdisk microresonator. *Sensors and Actuators B: Chemical*, *242*, 1115-1120.

Fabrication of optical fibre nanowires and their optical and mechanical characterisation. (2006). *42*(9), 517-519.

Fabrication of ultraviolet-curable adhesive bottle-like microresonators by wetting and photocuring. (2014). *Applied optics*, *53*(32), 7819-7824.

Universiti Malaya

Foreman, M. R., Swaim, J. D., & Vollmer, F. (2015). Whispering gallery mode sensors. *Advances in Optics and Photonics*, *7*(2), 168-240.

Giffney, T. J., Ng, Y., & Aw, K. (2011). A surface acoustic wave ethanol sensor with zinc oxide nanorods. *Smart Materials Research, 2012*.

Gorodetsky, M. L., Savchenkov, A. A., & Ilchenko, V. S. (1996). Ultimate Q of optical microsphere resonators. *Optics letters*, *21*(7), 453-455.

Gu, G., Guo, C., Cai, Z., Xu, H., Chen, L., Fu, H., Che, K., Hong, M., Sun, S., & Li, F. (2014). Fabrication of ultraviolet-curable adhesive bottle-like microresonators by wetting and photocuring. *Applied optics*, *53*(32), 7819-7824.

Hernaez, M., Mayes, A. G., & Melendi-Espina, S. (2018). Graphene oxide in lossy mode resonance-based optical fiber sensors for ethanol detection. *Sensors*, *18*(1), 58.

Isa, N. M., Irawati, N., Rahman, H. A., Yusoff, M. H., & Harun, S. W. (2018). Polyaniline Doped Poly (Methyl Methacrylate) Microfiber for Methanol Sensing. *IEEE Sensors Journal*.

Jali, M. H., Rahim, H. R. A., Ashadi, M. J. M., Thokchom, S., & Harun, S. W. (2018). Applied microfiber evanescent wave on ZnO nanorods coated glass surface towards temperature sensing. *Sensors and Actuators A: Physical*, *277*, 103-111.

Jali, M. H., Rahim, H. R. A., Hamid, S. S., Johari, M. A. M., Yusof, H. H. M., Thokchom, S., Harun, S. W., Khasanah, M., & Yasin, M. (2019). Microfiber loop resonator for formaldehyde liquid sensing. *Optik*, *196*, 163174.

Jiang, X., Yang, Q., Vienne, G., Li, Y., Tong, L., Zhang, J., & Hu, L. (2006). Demonstration of microfiber knot laser. *Applied Physics Letters*, *89*(14), 143513.

Johari, M., Al Noman, A., Khudus, M. A., Jali, M., Yusof, H., Harun, S., & Yasin, M. (2018). Microbottle resonator for formaldehyde liquid sensing. *Optik*, *173*, 180-184.

Johari, M. A. M., Al Noman, A., Khudus, M. A., Jali, M. H., Yusof, H. H. M., Harun, S. W., & Yasin, M. (2018). Microbottle resonator for formaldehyde liquid sensing. *Optik*, *173*, 180-184.

Universiti Malaya

Johari, M. A. M., Khudus, M. I. M. A., Jali, M. H. B., Al Noman, A., & Harun, S. W. (2019). Whispering Gallery Modes On Optical Micro-Bottle Resonator For Humidity Sensor Application. *Optik*.

Johari, M. A. M., Khudus, M. I. M. A., Jali, M. H. B., Maslinda, M., Ali, U. U. M., Harun, S. W., Zaidan, A., Apsari, R., & Yasin, M. (2019). Effect of tapering diameters with microbottle resonator for formaldehyde (CH2O) liquid sensing. *Sensing and Bio-Sensing Research*, *25*, 100292.

Johari, M. A. M., Pour, M. P., Al Noman, A., Khudus, M. I. M. A., Jali, M. H. B., Maslinda, M., Ali, U. U. M., & Harun, S. W. (2020). Effect of PMMA and PVA coating on the performance of optical microbottle resonator humidity sensors. *Microwave and Optical Technology Letters*, *62*(3), 993-998.

Kakarantzas, G., Dimmick, T., Birks, T., Le Roux, R., & Russell, P. S. J. (2001). Miniature all-fiber devices based on CO_2 laser microstructuring of tapered fibers. *Optics letters*, *26*(15), 1137-1139.

Kazanov, D., Poshakinskiy, A., Davydov, V. Y., Smirnov, A., Eliseyev, I., Kirilenko, D., Remškar, M., Fathipour, S., Mintairov, A., & Seabaugh, A. (2018). Multiwall MoS_2 tubes as optical resonators. *Applied Physics Letters*, *113*(10), 101106.

Kippenberg, T., Spillane, S., & Vahala, K. (2004). Demonstration of ultra-high-Q small mode volume toroid microcavities on a chip. *Applied Physics Letters*, *85*(25), 6113-6115.

Kokubun, Y. (2005). Wavelength selective integrated device by vertically coupled microring resonator filter. *Photonics Based on Wavelength Integration and Manipulation IPAP Books*, *2*, 303-316.

Konstantaki, M., Klini, A., Anglos, D., & Pissadakis, S. (2012). An ethanol vapor detection probe based on a ZnO nanorod coated optical fiber long period grating. *Optics express*, *20*(8), 8472-8484.

Kronenberg, P., Rastogi, P. K., Giaccari, P., & Limberger, H. G. (2002). Relative humidity sensor with optical fiber Bragg gratings. *Optics Letters*, *27*(16), 1385-1387.

Lee, H., Chen, T., Li, J., Yang, K. Y., Jeon, S., Painter, O., & Vahala, K. J. (2012). Chemically etched ultrahigh-Q wedge-resonator on a silicon chip. *Nature photonics*, *6*(6), 369-373.

Universiti Malaya

Lee, P.-T., Lu, T.-W., Fan, J.-H., & Tsai, F.-M. (2007). High quality factor microcavity lasers realized by circular photonic crystal with isotropic photonic band gap effect. *Applied physics letters*, *90*(15), 151125.

Lee, P.-T., Lu, T.-W., Tsai, F.-M., & Lu, T.-C. (2006). Investigation of whispering gallery mode dependence on cavity geometry of quasiperiodic photonic crystal microcavity lasers. *Applied physics letters*, *89*(23), 231111.

Liang, L., Li, M., Liu, N., Sun, H., Rong, Q., & Hu, M. (2018). A high-sensitivity optical fiber relative humidity sensor based on microsphere WGM resonator. *Optical Fiber Technology*, *45*, 415-418.

Liang, W., Huang, Y., Xu, Y., Lee, R. K., & Yariv, A. (2005). Highly sensitive fiber Bragg grating refractive index sensors. *Applied Physics Letters*, *86*(15), 151122.

Lim, K., Harun, S., Arof, H., & Ahmad, H. (2012a). Fabrication and applications of microfiber. *Selected Topics on Optical Fiber Technology*, 473-508.

Lim, K., Harun, S., Arof, H., & Ahmad, H. (2012b). Fabrication and applications of microfiber. In *Selected Topics on Optical Fiber Technology*. InTech.

Louyer, Y., Meschede, D., & Rauschenbeutel, A. (2005). Tunable whispering-gallery-mode resonators for cavity quantum electrodynamics. *Physical Review A*, *72*(3), 031801.

Low-loss highly overcoupled fused couplers: Fabrication and sensitivity to external pressure. (1988). *6*(10), 1476-1482.

Matsko, A. B., & Ilchenko, V. S. (2006a). Optical resonators with whispering-gallery modes-part I: basics. *IEEE Journal of selected topics in quantum electronics*, *12*(1), 3-14.

Matsko, A. B., & Ilchenko, V. S. (2006b). Optical resonators with whispering gallery modes I: basics. *IEEE J. Sel. Top. Quantum Electron*, *12*(3), 3.

Md Ashadi, M. J., Muhammad Imran Mustafa, A. K., Mohd Hafiz, J., Abdullah, A. N., & Sulaiman Wadi, H. (2019). Microbottle resonator for temperature sensing. Journal of Physics: Conference Series,

Mignani, A. G., Falciai, R., & Ciaccheri, L. (1998). Evanescent wave absorption spectroscopy by means of bi-tapered multimode optical fibers. *Applied Spectroscopy*, *52*(4), 546-551.

Universiti Malaya

Miniature all-fiber devices based on CO 2 laser microstructuring of tapered fibers. (2001). *Optics Letters*, *26*(15), 1137-1139.

Murugan, G. S., Petrovich, M., Jung, Y., Wilkinson, J., & Zervas, M. (2011). Hollow-bottle optical microresonators. *Optics express*, *19*(21), 20773-20784.

Murugan, G. S., Wilkinson, J. S., & Zervas, M. N. (2009). Selective excitation of whispering gallery modes in a novel bottle microresonator. *Optics express*, *17*(14), 11916-11925.

Nasir, M. N. M., Murugan, G. S., & Zervas, M. N. (2016a). Broadly tunable solid microbottle resonator. Photonics Conference (IPC), 2016 IEEE,

Nasir, M. N. M., Murugan, G. S., & Zervas, M. N. (2016b). Spectral cleaning and output modal transformations in whispering-gallery-mode microresonators. *JOSA B*, *33*(9), 1963-1970.

Near-field characterization of glass microfibers on a low-index substrate. (2010). *Applied Physics B*, *101*(1-2), 291-295.

Optical fiber nanowires and microwires: a review. (2010). *12*(4), 043001.

Optical fibre nanotaper sensors. (2010). *Optical fiber technology*, *16*(6), 331-342.

Optical microfibers and nanofibers. (2013). *Nanophotonics*, *2*(5-6), 407-428.

Pauzi, N., Man, S., Nawawi, M. S. A. M., & Abu-Hussin, M. F. B. (2019). Ethanol standard in halal dietary product among Southeast Asian halal governing bodies. *Trends in Food Science & Technology*.

Photonics nanowires directly drawn from bulk glasses. (2006). *14*(1), 82-87.

Pöllinger, M., O'Shea, D., Warken, F., & Rauschenbeutel, A. (2009). Ultrahigh-Q tunable whispering-gallery-mode microresonator. *Physical review letters*, *103*(5), 053901.

Punjabi, N., Satija, J., & Mukherji, S. (2015). Evanescent wave absorption based fiber-optic sensor-cascading of bend and tapered geometry for enhanced sensitivity. In *Sensing Technology: Current Status and Future Trends III* (pp. 25-45). Springer.

Universiti Malaya

Rayleigh, L. (1910). CXII. The problem of the whispering gallery. *The London, Edinburgh, and Dublin Philosophical Magazine and Journal of Science*, *20*(120), 1001-1004.

Roshan, H., & Sheikhi, M. H. (2020). A novel room temperature ethanol sensor based on PbS: SnS2 nanocomposite with enhanced ethanol sensing properties. *Journal of Alloys and Compounds*, *816*, 152666.

Savchenkov, A. A., Matsko, A. B., Ilchenko, V. S., & Maleki, L. (2007). Optical resonators with ten million finesse. *Optics express*, *15*(11), 6768-6773.

Self-modulated taper drawing of silica nanowires. (2005). *16*(9), 1445.

The shape of fiber tapers. (1992). *10*(4), 432-438.

Srinivasan, K., & Painter, O. (2007). Optical fiber taper coupling and high-resolution wavelength tuning of microdisk resonators at cryogenic temperatures. *Applied Physics Letters*, *90*(3), 031114.

Sumetsky, M. (2004a). Optical fiber microcoil resonator. *Optics express*, *12*(10), 2303-2316.

Sumetsky, M. (2004b). Whispering-gallery-bottle microcavities: the three-dimensional etalon. *Optics letters*, *29*(1), 8-10.

Sumetsky, M. (2017). Lasing microbottles. *Light: Science & Applications*, *6*(10), e17102-e17102.

Sumetsky, M., DiGiovanni, D., Dulashko, Y., Fini, J., Liu, X., Monberg, E., & Taunay, T. (2011). Surface nanoscale axial photonics: robust fabrication of high-quality-factor microresonators. *Optics letters*, *36*(24), 4824-4826.

Sumetsky, M., Dulashko, Y., Fini, J. M., & Hale, A. (2005). Optical microfiber loop resonator. *Applied Physics Letters*, *86*(16), 161108.

Theoretical analysis and fabrication of tapered fiber. (2013). *Optik*, *124*(6), 538=543.

Universiti Malaya

Tian, X., Powell, K., Li, L., Chew, S. X., Yi, X., Nguyen, L., & Minasian, R. A. (2020). High-Resolution Optical Microresonator-Based Sensor Enabled by Microwave Photonic Sidebands Processing. *Journal of Lightwave Technology*, *38*(19), 5440-5449.

Vahala, K. J. (2003a). Optical microcavities. *Nature*, *424*(6950), 839-846.

Vahala, K. J. (2003b). Optical microcavities. *Nature*, *424*(6950), 839.

Vollmer, F., Braun, D., Libchaber, A., Khoshsima, M., Teraoka, I., & Arnold, S. (2002). Protein detection by optical shift of a resonant microcavity. *Applied Physics Letters*, *80*(21), 4057-4059.

Vollmer, F., & Yang, L. (2012). Review Label-free detection with high-Q microcavities: a review of biosensing mechanisms for integrated devices. *Nanophotonics*, *1*(3-4), 267-291.

Ward, J. M., O'Shea, D. G., Shortt, B. J., Morrissey, M. J., Deasy, K., & Nic Chormaic, S. G. (2006). Heat-and-pull rig for fiber taper fabrication. *Review of Scientific Instruments*, *77*(8), 083105.

Warken, F., Rauschenbeutel, A., & Bartholomaus, T. (2008). Fiber Pulling Profits from Precise Positioning-Precise motion control improves manufacturing of fiber optical resonators. *Photonics Spectra*, *42*(3), 73.

White, I. M., Oveys, H., & Fan, X. (2006). Liquid-core optical ring-resonator sensors. *Optics letters*, *31*(9), 1319-1321.

Wu, X., & Tong, L. (2013). Optical microfibers and nanofibers. *Nanophotonics*, *2*(5-6), 407-428.

Xu, L., Fanguy, J. C., Soni, K., & Tao, S. (2004). Optical fiber humidity sensor based on evanescent-wave scattering. *Optics Letters*, *29*(11), 1191-1193.

Yang, J., Huang, M., Dai, X., Huang, M., & Liang, Y. (2013). A spoof surface WGM sensor based on a textured PEC cylinder. *EPL (Europhysics Letters)*, *103*(4), 44001.

Yin, Y., Niu, Y., Dai, L., & Ding, M. (2018). Cascaded microbottle resonator and its application in add–drop filter. *IEEE Photonics Journal*, *10*(4), 1-10.

Universiti Malaya

Yusof, H. H. M., Jali, M. H., Johari, M. A. M., Dimyati, K., Harun, S. W., Khasanah, M., & Yasin, M. (2019). Detection of formaldehyde vapor using glass substrate coated with zinc oxide nanorods. *IEEE Photonics Journal*, *11*(1), 1-9.

Zhang, M., Buscaino, B., Wang, C., Shams-Ansari, A., Reimer, C., Zhu, R., Kahn, J. M., & Lončar, M. (2019). Broadband electro-optic frequency comb generation in a lithium niobate microring resonator. *Nature*, *568*(7752), 373-377.

Universiti Malaya